

# **Computational and Matrix Isolation Infrared Spectroscopic Studies of Dehydrobenzylalcohol Radicals**

**Lincoln  
MS15076**

**A dissertation submitted for the partial fulfillment  
of BS-MS dual degree in Science**

**Indian Institute of Science Education and Research Mohali  
April 2020**



# CERTIFICATE OF EXAMINATION

This is to certify that the dissertation titled “**Computational Studies of Dehydrobenzyl derivatives and Matrix Isolation Infrared Spectroscopic Studies of 2-Dehydrobenzylalcohol Radicals**” submitted by Mr. Lincoln (Registration Number: MS15076) for the partial fulfillment of BS-MS dual degree program of Indian Institute of Science Education and Research, Mohali, has been examined by the thesis committee duly appointed by the institute. The committee finds the work done by the candidate satisfactory and recommends that the report be accepted.

Dr. Sugumar Venkataramani  
(Supervisor)

Dr. Jino George  
(Committee member)

Dr. P. Balanarayan  
(Committee member)

Date: 3<sup>rd</sup> May, 2020

# DECLARATION

The work presented in this dissertation has been carried out by me under the guidance of Dr. Sugumar Venkataramani at the Indian Institute of Science Education and Research, Mohali. This work has not been submitted in part or in full for a degree, a diploma, or a fellowship to any university or institute. Whenever contributions of others are involved, every effort is made to indicate this clearly, with due acknowledgment of collaborative research and discussion. This thesis is a bonafide record of original work done by me and all sources listed within have been detailed in the bibliography.

Lincoln  
(Candidate)

Dated: 3<sup>rd</sup> May, 2020

In my capacity as the supervisor of the candidate's project work, I certify that the above statements by the candidate are true to the best of my knowledge.

Dr. Sugumar Venkataramani  
(Supervisor)

# ACKNOWLEDGEMENT

Firstly, I would like to express my special thanks of gratitude towards my MS thesis supervisor Dr. Sugumar Venkataramani, who gave me the golden opportunity in his lab to pursue research work and his help, able guidance, immense support. I would also like to thank Dr. P. Balanarayan and Dr. Jino George for being a part of my thesis committee and giving their valuable suggestions throughout the year and during my presentations. I would like to extend my thanks to our past director prof. N. Satyamurthi, prof. Arvind, current director prof. J. Gowrishankar, Dr. S. Arulananda Babu, Head of the Department, chemistry for their cooperation and mentorship during this whole experience. Special mention to prof. K. S. Viswanathan for always helping me out and giving me an opportunity to work with him.

Secondly, I would like to thank all my group members including Mayank Saraswat, Anjali Mahadevan, Chitranjan Sah, Amandeep Singh, Virinder Bhagat, Ankit Somani, Ajit Yadav, Sapna, Debpriya, Himanshu Kumar, Ankit, Pravesh Kumar, Surbhi Grewal, Anjali, Sonam.

I would like to specially thank Mayank Saraswat for his invaluable help during my research days. I would not have been able to complete my research work without his suggestions and guiding me to apply for Ph.D, to Anjali Mahadevan for her ideas and help in poster and thesis, to Chitranjan Sah for entertainment, and to Amandeep Singh for being with me emotionally and academically.

My special thanks to all of my friends including Nevil U Shah, Megha Dhiman, Prashant Nagar, Lopamudra Das, Hunarpreet Kaur, Bhumija Gautam, Harjasnoor Kakkar, Vishal Gaur, Perna Goel, Geetika Aggarwal, Sneha Bisht for helping me get through my IISER life. I would extend my special thanks towards Nevil U Shah, Sneha Bisht for being always there for all the time. I want to thank Vishal and Perna for the outings and Megha, Prashant and Lopa for the tea breaks.

Furthermore, I would like to extend my gratitude and thanks to my mother and father for caring about me and helping me throughout my life. Special mention to my sister for listening to me always and her belief in me. I would like to thank all the teachers and friends in my life too. This journey would not have been possible without all these people.

Lastly, I would like to thank IISER Mohali for computational facilities, all other technical and non-technical staff and KVPY for providing me with financial help.

# CONTENTS

List of Abbreviations	i
List of Figures	iii
List of Tables	vii
List of Schemes	viii
Abstract	ix
<b>Chapter 1. Introduction</b>	<b>1</b>
<b>Chapter 2. Results and Discussion</b>	<b>6</b>
2.1 Computational Studies	6
2.1.1 Understanding Electronic Structure of Dehydrobenzyl Derivatives.	6
2.1.2 Thermal Reactivity Studies	18
2.2 Matrix Isolation Infrared Spectroscopic Studies on 2-Iodobenzylalcohol	24
2.2.1 Experiment in Argon Matrix	24
<b>Chapter 3. Conclusions and Perspectives</b>	<b>34</b>
<b>Chapter 4. Materials and Methods</b>	<b>36</b>
4.1 Computational Details	36
4.1.1 Methods in Computational Chemistry	36
4.1.2 Basis Sets	37

4.1.3 Geometry Optimization and Frequency Calculation	39
4.1.4 Thermochemistry	40
4.2 Experimental Set-up	40
4.2.1 Matrix Isolation Technique	40
4.2.2 Frequency Shift	41
4.2.3 Set-up of Matrix Isolation Technique and its Functioning	41
4.2.4 Matrix Isolation FT-IR Facility in POC Lab at IISER Mohali	44
<b>Chapter 5. References</b>	<b>45</b>
<b>Appendix 1. Electronic Structures Parameters of Selected Species</b>	<b>48</b>
<b>Appendix 2. Experimental and computational infrared data of 2-iodobenzylalcohol</b>	<b>49</b>
<b>Appendix 3. Cartesian Co-ordinates of Selected Species</b>	<b>51</b>

# LIST OF ABBREVIATIONS

**PED** Potential Energy Diagram

**IR** Infra-red

**POC** Physical Organic Chemistry

*o* *ortho-*

*m* *meta-*

*p* *para-*

**K** Kelvin

**MI** Matrix Isolation

**BDE** Bond Dissociation Energy

**RSE** Radical Stabilization Energy

**TS** Transition State

**DFT** Density Functional Theory





# LIST OF FIGURES

- Figure 1.1** Major conformers of benzylalcohol
- Figure 1.2** Schematic description of matrix isolated 2-iodobenzylalcohol in argon matrix
- Figure 2.1(a)** Geometrical parameters (bond angle in degrees and bond distances in Å) of benzylalcohol (**1**), and all different possible radical isomers (**1a**, **1b**, **1c**, **1d** and **1e**). Bold: (U)B3LYP/cc-pVTZ, Normal: (U)M06-2X/cc-PVTZ levels of theory.
- Figure 2.1(b)** Geometrical parameters (bond angle in degrees and bond distances in Å) of benzylmercaptan (**2**), and all different possible radical isomers (**2a**, **2b**, **2c**, **2d** and **2e**). Bold: (U)B3LYP/cc-pVTZ, Normal: (U)M06-2X/cc-PVTZ levels of theory.
- Figure 2.2(a)** Spin density values at (U)B3LYP/cc-pVTZ (bold), (U)M06-2X/cc-PVTZ levels of theory, and molecular orbitals corresponding to SOMO for the dehydrobenzylalcohol radical isomers (level of theory and the molecular orbitals are rendered at an isovalue 0.05).
- Figure 2.2(b)** Spin density values at (U)B3LYP/cc-pVTZ (bold), (U)M06-2X/cc-PVTZ levels of theory, and molecular orbitals corresponding to SOMO for the dehydrobenzylmercaptan radical isomers (level of theory and the molecular orbitals are rendered at an isovalue 0.05).
- Figure 2.3(a)** Potential energy diagrams corresponding to the 1,2-, 1,3- and 1,4-H-shifts in **1a**, **1b**, **1c**, **1d** and **1e** (reactant, corresponding TS and corresponding

product) calculated at (U)B3LYP/cc-pVTZ (bold) and (U)M062X/cc-pVTZ (normal font) levels of theory.

**Figure 2.3(b)** Potential energy diagrams corresponding to the 1,2-, 1,3- and 1,4-H-shifts in **2a**, **2b**, **2c**, **2d** and **2e** (reactant, corresponding TS and corresponding product) calculated at (U)B3LYP/cc-pVTZ (bold) and (U)M062X/cc-pVTZ (normal font) levels of theory.

**Figure 2.4(a)** Potential energy diagrams corresponding to the ring-opening and fragmentation of **1a**, **1b**, and **1c** (reactant, corresponding TS and corresponding product) calculated at (U)B3LYP/cc-pVTZ (bold) (U)M062X/cc-pVTZ (normal font) levels of theory.

**Figure 2.4(b)** Potential energy diagrams corresponding to the ring-opening and fragmentation of **2a**, **2b**, and **2c** (reactant, corresponding TS and corresponding product) calculated at (U)B3LYP/cc-pVTZ (bold) (U)M062X/cc-pVTZ (normal font) levels of theory.

**Figure 2.5** Deposition spectra of 2-iodobenzylalcohol in argon matrix at 4 K (region wise): **(a)** 1650 – 550  $\text{cm}^{-1}$ ; & **(b)** 3800 – 2800  $\text{cm}^{-1}$ .

**Figure 2.6** Major conformers of 2-iodobenzylalcohol

**Figure 2.7** **(a)** Deposition spectrum of 2-iodobenzylalcohol in argon matrix at 4 K (region wise): **(top)** 1650 – 550  $\text{cm}^{-1}$ ; & **(bottom)** 3800 – 2800  $\text{cm}^{-1}$ ; **(b, c & d)** Calculated spectrum of conformers **1**, **2**, **3** and **4**, respectively (B3LYP/DGTZVP, unscaled).

**Figure 2.8** **(a)** Deposition spectrum of 2-iodobenzylalcohol in argon matrix at 4 K (region wise): **(top)** 1650 – 550  $\text{cm}^{-1}$ ; & **(bottom)** 3800 – 2800  $\text{cm}^{-1}$ ; **(b)**

Difference spectrum after irradiation at 365 nm (c) Difference spectrum after irradiation at 254 nm (signals pointing upward direction signifies the formation of new species and those pointing downward disappear upon irradiation).

**Figure 2.9** Potential energy surface (PES) scan for 2-iodobenzylalcohol upon changing the dihedral angle C-C-C-O. PES scan from Conformer **1** to Conformer **3** (a) at B3LYP/cc-pVTZ; (b) at M06-2X/cc-pVTZ; PES scan from Conformer **2** to Conformer **4** (c) at B3LYP/cc-pVTZ; (d) at M06-2X/cc-pVTZ.

**Figure 2.10:** Two possible mechanisms for the light induced conformational changes in 2-iodobenzylalcohol (a) Excited State Conformational Changes; (b) Hot Ground State Conformational Changes

**Figure 4.1** Matrix isolation set-up.



# LIST OF TABLES

- Table 2.1(a)** Relative energies (kcal/mol) of dehydrobenzylalcohol isomeric radicals at (U)B3LYP/cc-pVTZ, (U)M06-2X/cc-pVTZ and CBS-QB3 level of theory.
- Table 2.1(b)** Relative energies (kcal/mol) of dehydrobenzylmercaptan isomeric radicals at (U)B3LYP/cc-pVTZ, (U)M06-2X/cc-pVTZ and CBS-QB3 level of theory.
- Table 2.2(a)** Bond Dissociation Energies (BDEs) of first homolytic C-H bond (in kcal/mol) of dehydrobenzylalcohol radical isomers.
- Table 2.2(b)** Bond Dissociation Energies (BDEs) of first homolytic C-H bond (in kcal/mol) of dehydrobenzylmercaptan radical isomers.
- Table 2.3(a)** Radical stabilization energies (RSEs) (in kcal/mol) of dehydrobenzylalcohol isomeric radicals calculated using isodesmic reaction.
- Table 2.3(b)** Radical stabilization energies (RSEs) (in kcal/mol) of dehydrobenzylmercaptan isomeric radicals calculated using isodesmic reaction.
- Table 2.4** Relative energy and relative Boltzmann populations (in the parenthesis) of possible conformers of 2-iodobenzylalcohol at different level of theory.

# LIST OF SCHEMES

- Scheme 1.1** Photodissociation dynamics of benzylalcohol at 193nm
- Scheme 1.2** Schematic representation of 1,2-H atom rearrangements in benzyloxy radicals
- Scheme 2.1(a)** Possible radical isomers (**1a-d**: C-centered and **1e**: O-centered) of benzylalcohol
- Scheme 2.1(b)** Possible radical isomers (**2a-d**: C-centered and **2e**: S-centered) of benzylmercaptan

# Abstract

Benzyloxyl radical is an important reactive intermediate in the oxidation of toluene and other substituted aromatic hydrocarbons. The benzyloxyl radical is expected to promptly decompose to new products like benzaldehyde and benzene. Despite the experimental exploration of kinetics and product branching ratios of decomposition channel of benzyloxy radical, the isomerization pathways of benzyloxyl to other radical isomers and its unimolecular decomposition pathways have not been well investigated. In this work, we explore the isomerization and decomposition pathways of benzyloxyl radical using computational methods. To get additional insights into the effect of replacement of sulfur with oxygen, we have also explored the benzylthiyl radical isomers as well as their isomeric phenyl radical isomers.

Furthermore, the target benzyloxy radical was intended to generate under photochemical conditions using 2-iodobenzylalcohol as a precursor isolated in argon matrix at 4 K. A possible isomerization of the 2-dehydrobenzylalcohol (formed from photo irradiation) to benzyloxyl radical through 1,4-H shift was expected in the further photochemistry of the benzyloxyl radical. Surprisingly, our experimental investigations led to light-induced conformational changes of 2-iodobenzylalcohol instead of the radical in argon matrix. Both these computational and experimental results are discussed in the thesis in detail.



# Chapter 1. Introduction

## 1.1 General Introduction to Radicals

Radicals are one of the most important species in the field of chemistry, but their nature is very reactive except some (e.g. (2,2,6,6-Tetramethylpiperidin-1-yl)oxyl (i.e. TEMPO), Verdazyl radicals, etc.)<sup>[1,2]</sup>, due to which their characterization has posed some real challenges. Any chemical species can be considered to be a radical if it contains one or more unpaired valence electron(s), which is responsible for its reactive nature. Under standard conditions, they tend to dimerize spontaneously to form a stable species. Their lifetime is very short, so their characterization has been one of the biggest challenges for the chemists. Their characterization is necessary as it is present in various aspects such material chemistry, petrochemistry, biomolecular chemistry as well as organic reactions. Radical chemistry has a vital role to play in combustion, for ignition and pyrolysis for rapid rates of reaction<sup>[3]</sup>. Additionally, their use in the field of polymer chemistry is undeniably significant as without the formation of radicals, reactions like RAFT<sup>[4-7]</sup> (Reversible Addition Fragmentation Chain Transfer), ATRP (Atom Transfer Radical Polymerization) won't proceed. Photodissociation of CFCs (Chlorofluorocarbons) gives chlorine radicals, which in turn depletes the ozone layer posing various health problems and solving this problem is of great interest to atmospheric chemists<sup>[8-10]</sup>. The importance of radicals is not just limited to the field of chemistry but has a vital role in biological areas also. These are involved in the cell signaling process called redox signaling<sup>[11]</sup>. They have a role to play in some of the diseases like Parkinson's disease, Schizophrenia, and Alzheimer's<sup>[12]</sup> also. The most common type of cell damage is associated with reactive oxygen species (ROS), which contains superoxide, hydrogen peroxide, and hydroxyl radicals. These types of radicals are responsible for cell death in excess because of their reactivity, which could lead to unwanted side reactions. These cell deaths are responsible for contributing to disease like cancer, diabetes, strokes, myocardial infarction<sup>[13]</sup>. The reactions between radicals and DNA could possibly result in mutations and could potentially be a reason for many types of cancer<sup>[14]</sup>.

Due to the presence of unpaired electron, radicals possess paramagnetic property. Radicals can be identified and characterized using ESR (Electron Spin Resonance) technique, which is being used

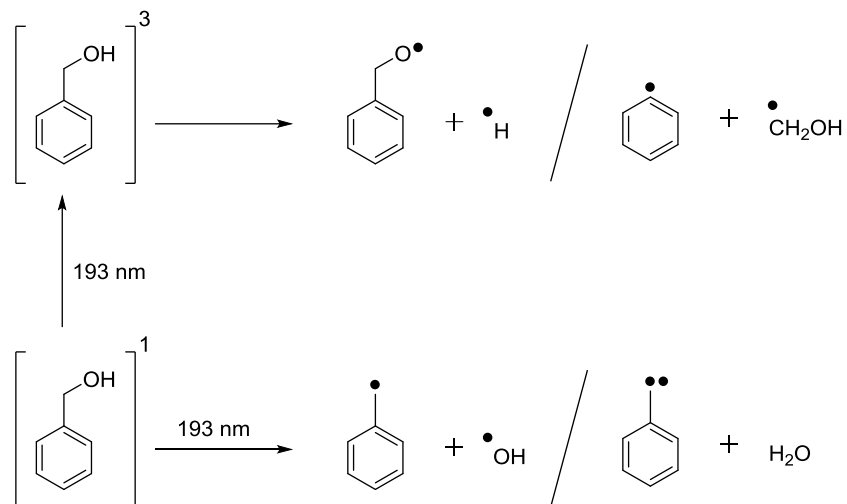
worldwide. With certain limitation, other spectroscopic techniques have also been employed to study the radical chemistry. Matrix isolation is the one of the common techniques used to trap and study the radicals using different spectroscopic techniques in conjugation.

Formation of radicals can be spontaneous or could be a result of external factors like heat, light, etc. The creation of reactive intermediates from their precursor molecules can be broadly categorized into two ways: (i) Photochemical pathway: Irradiating the precursor molecule with the light of appropriate wavelength; (ii) Thermal pathway: Providing enough heat to the precursor molecule may lead to the homolytic cleavage of specific bonds or fragmentation to byproducts.

## 1.2 Literature Background

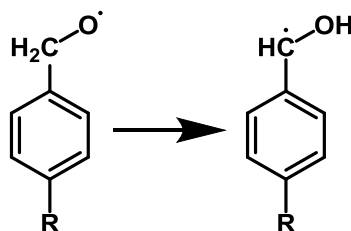
During the last 50 years, many studies have been done to characterize various radicals. The system of our interest is benzyloxy radical on which few studies have been carried out recently.

Benzyloxy radical is an important intermediate in the oxidation of toluene and other substituted aromatic hydrocarbons<sup>[15]</sup>. The benzyloxy radical is expected to promptly decompose to new products like benzaldehyde and benzene. The kinetics and product branching ratios of benzyloxy radical decomposition over a wide range of temperature and pressure conditions, to improve kinetic models for the oxidation of aromatic hydrocarbon has been explored by Bozelli and coworkers<sup>[16]</sup>. Wei-Ping Hu and his co-workers investigated the photodissociation dynamics of benzylalcohol at 193 nm<sup>[17]</sup>. In this report, they have used multimass ion imaging technique using VUV laser for ionization at 193 nm. They observed four dissociation channels, which they verified using time of flight (TOF) mass spectrometry (**Scheme 1.1**). They found different signals at  $m/z = 77, 79, 89, 91, 105$ , which correspond to phenyl radical,  $C_6H_7^+$ ,  $C_7H_5^+$ , benzyl radical, and a carbene, respectively. First channel was the OH elimination channel, in which a sharp line with  $m/z = 91$  was observed that represents the fragmentation of OH and formation of stable benzylic radical. The next channel was  $H_2O$  elimination channel with a sharp peak at  $m/z = 89$  because of  $C_7H_5^+$ . Third pathway follows through the elimination of H, which leads to the formation of  $C_7H_7O$ . Further using 118 nm UV light, it forms  $C_6H_7^+$ , losing CO in the process, with intense peak at  $m/z = 79$ . Last elimination channel consists of losing  $CH_2OH$  giving rise to an intense peak at  $m/z = 77$  for  $C_6H_5$ .



**Scheme 1.1:** Photodissociation dynamics of benzylalcohol at 193 nm

In another work done by Shubham Vyas and his co-workers, rearrangement through 1,2-H atom shifts in benzyloxy radicals have been explored<sup>[18]</sup>. The authors have tried to find the effect of solvents on the rate of 1,2-H atom rearrangement in *para*-substituted benzyloxy radicals using density functional theory (DFT) (**Scheme 1.2**). Furthermore, they tried changing the *para* substitution with electron-donating and electron-withdrawing groups to perceive the change in the rate of radical rearrangement. Moreover, the rate of radical rearrangement was considerably influenced by the presence of implicit as well as explicit solvents. The rate was found to be dependent on the spatial distance between the rearranging hydrogen atom and carbon atom present in the transition state. In this report, it was shown that this distance could be modified accordingly by the presence of *para* substituent and solvent molecules.



**Scheme 1.2:** Schematic representation of 1,2-H atom rearrangements in benzyloxy radicals

Furthermore, presence of different benzylalcohol conformers were confirmed using UV and IR-UV Ion Dip Spectroscopy<sup>[19]</sup>. According to the report, there are two different conformers present for benzylalcohol namely *gauche* (*g*) and *trans* (*t*). These conformers arise by doing *ab initio* calculations for potential energy scan (PES) by varying the dihedral angle of C-C-C-O, which led to the availability of two minima – *g* and *t*. They observed that conformer *g* was energetically more stable than conformer *t* by a very small energy barrier. The two different conformers are shown in the **figure 1.1**.

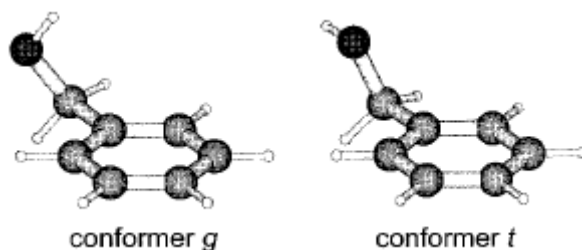


**Figure 1.1:** Major conformers present for benzylalcohol.

### 1.3 Overview of Matrix Isolation Technique

The origin of the matrix isolation technique went to the start of the 20th century and was developed by the pioneers of the fields - George C. Pimentel - during the 1950s. This technique attracted the attention of people because of its advantage in trapping and characterization of radicals and other open-shell systems. The principle behind this technique is to trap the reactive intermediates inside the matrix gases like nitrogen, helium, argon, etc., which are chemically unreactive or inert to the precursor molecule. The concentration used for the precursor molecule to host gas is typically in the range of 1:1000 to 1:2000. The host gas is taken in large excess so that the intermolecular interactions between the precursor molecules are negligible. Many spectroscopic techniques (like UV-Vis, NMR, FTIR, and EPR) can be attached to this matrix isolation setup for the analysis and characterization of radicals. This technique has some advantages over other techniques as the molecule gets trapped inside the matrix at very low temperature, and so the translational and rotational motions get hindered. The peak we get is narrow because of negligible collisional and Doppler broadening. This technique has some disadvantages also as we cannot study the formation and decay rates of the reactive intermediates as in the case of time-resolved spectroscopy. Because of the hindrance of rotations by the solid cages, we do not get the rotational spectrum. The

experimental spectrum can be rationalized by comparing with the computationally predicted spectra, which are generally shifted due to the cage constraints. In general, computationally predicted spectra are of gas-phase molecules, whereas the values of frequency in the experimental spectrum are shifted because of van der Waals, electrostatic, and repulsive interactions between the host and guest molecules.

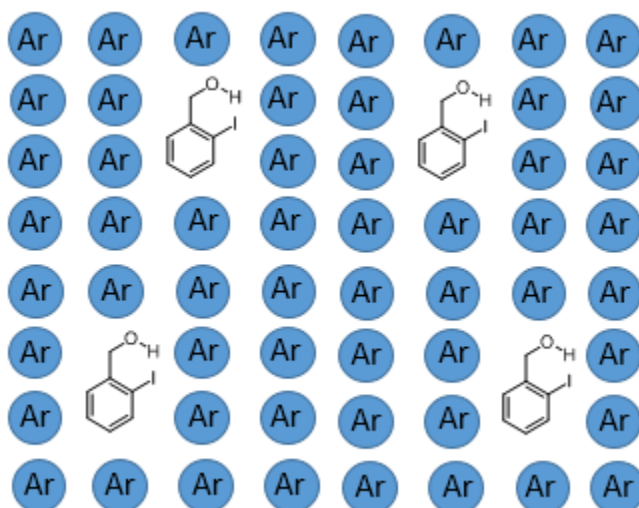


**Figure 1.2:** Schematic description of matrix isolated 2-iodobenzylalcohol in argon matrix

#### 1.4 Our Approach

The main purpose of our work was to trap and stabilize benzyloxyl radicals under cryogenic conditions using matrix isolation IR technique. In this regard, computational investigations on electronic structure, stability and reactivity aspects of the benzyloxyl radical and all its possible phenyl radical isomers have been set as the first part of the thesis. Essentially, we have endeavored to explore the reactivity aspects related to isomerization and decomposition pathways of benzyloxyl radical using computational methods. Along the line, the effect of replacement of sulfur with oxygen, we have also explored the similar studies on benzylthiyl radical and its analogous phenyl radical isomers. In the second part of the thesis, experimental studies were performed on 2-iodobenzylalcohol with the set goal in achieving benzyloxyl radical through the photochemical generation 2-hydroxymethylphenyl radical, followed by a 1,4-H shift. Surprisingly, the experimental results were not what we anticipated. Instead of our target radical formation photochemistry, we observed a light induced conformational changes.

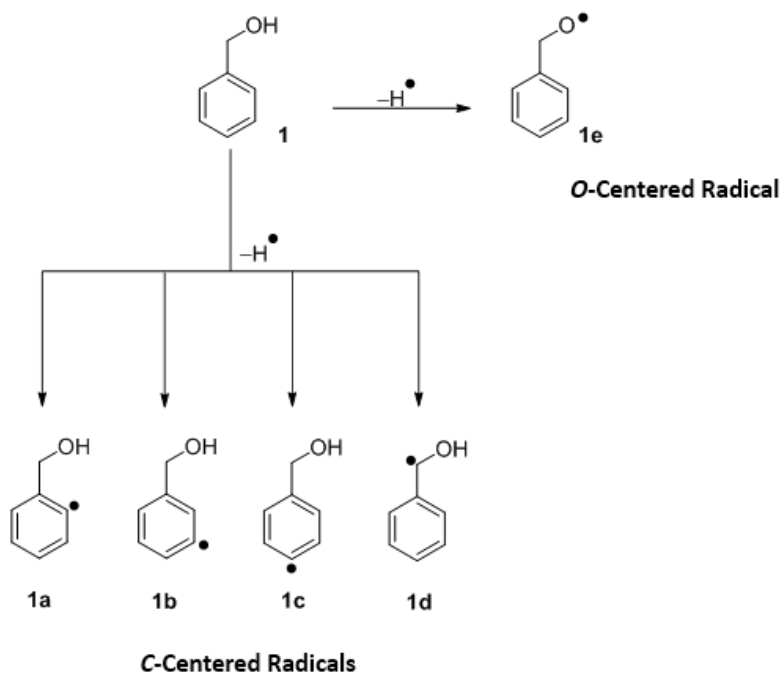
## Chapter 2. Results and Discussion

### 2.1 Computational Studies

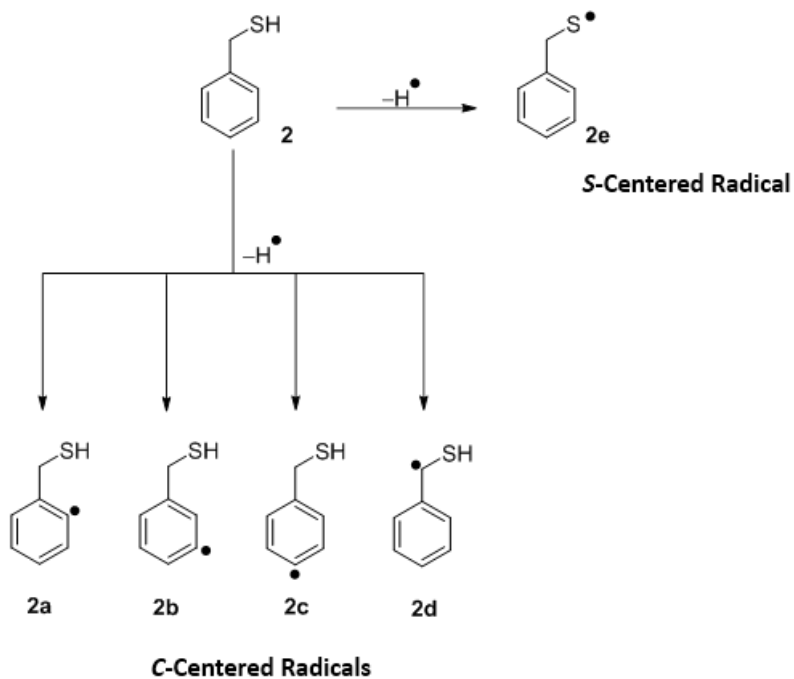
Computational studies on dehydroradical isomers of benzylalcohol and benzylmercaptan were carried out. The major goal in this regard is towards understanding electronic structural, (geometrical and conformational preferences, spin densities and molecular orbitals), and stability order (thermodynamic stability) through computations. Furthermore, reactivity studies are done for benzylalcohol and benzylmercaptan radical isomers, including the unimolecular decomposition channels to throw light on the kinetic stability of radical isomers. Reactivity studies are expanded to hydrogen shifts, which includes 1,2-, 1,3-, and 1,4-H-shifts for dehydroradical isomers of benzylalcohol and benzylmercaptan. The electronic structural studies and reactivity pathways have been discussed in details in this chapter.

#### 2.1.1 System of Interest

Five radical isomers are possible by the cleavage of C-H bond and one radical isomer by the cleavage of O-H and S-H bond for benzylalcohol and benzylmercaptan, respectively (**Scheme 2.1a,b**). The C-centered radicals have been named as **a-d** according to their position. The *ortho*, *meta* and *para* are named as **a**, **b** and **c**, respectively and the benzyl radical is named **d**. The heteroatom centered radical is named **e**.



**Scheme 2.1a:** Possible radical isomers (**1a-d**: C-centered and **1e**: O-centered) of benzylalcohol



**Scheme 2.1b:** Possible radical isomers (**2a-d**: C-centered, **2e**: S-centered) of benzylmercaptan.

## 2.1.2 Geometrical Parameters

Structural optimization was carried out for all possible radical isomers of benzylalcohol and benzylmercaptan at (U)B3LYP/cc-pVTZ and (U)M06-2X/cc-pVTZ (**Figure 2.1a,b**). Based on the geometries of the radical isomers, it was observed that the bond angle at the radical center increased as compared to the parent molecule. We found out that there was an increase in approximately  $5^{\circ}$ - $6^{\circ}$  in the bond angle at the phenylic radical center but  $12^{\circ}$ - $14^{\circ}$  at the benzylic radical, than the parent molecule. These results were consistent for all the radical centers for benzylalcohol and benzylmercaptan.

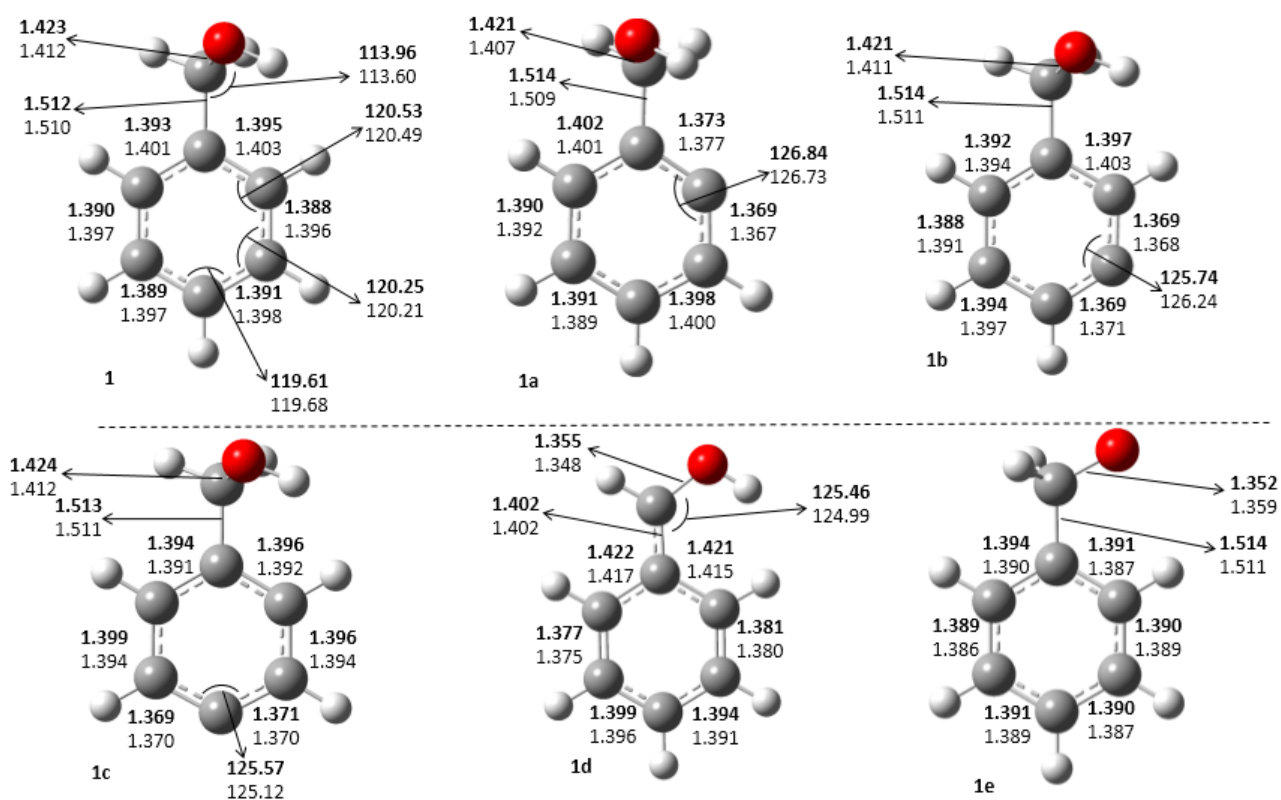


**Figure 2.1a.** Geometrical parameters (bond angle in degrees and bond distances in Å) of benzylalcohol (**1**), and all different possible radical isomers (**1a**, **1b**, **1c**, **1d** and **1e**). Bold: (U)B3LYP/cc-pVTZ, Normal: (U)M06-2X/cc-PVTZ levels of theory.



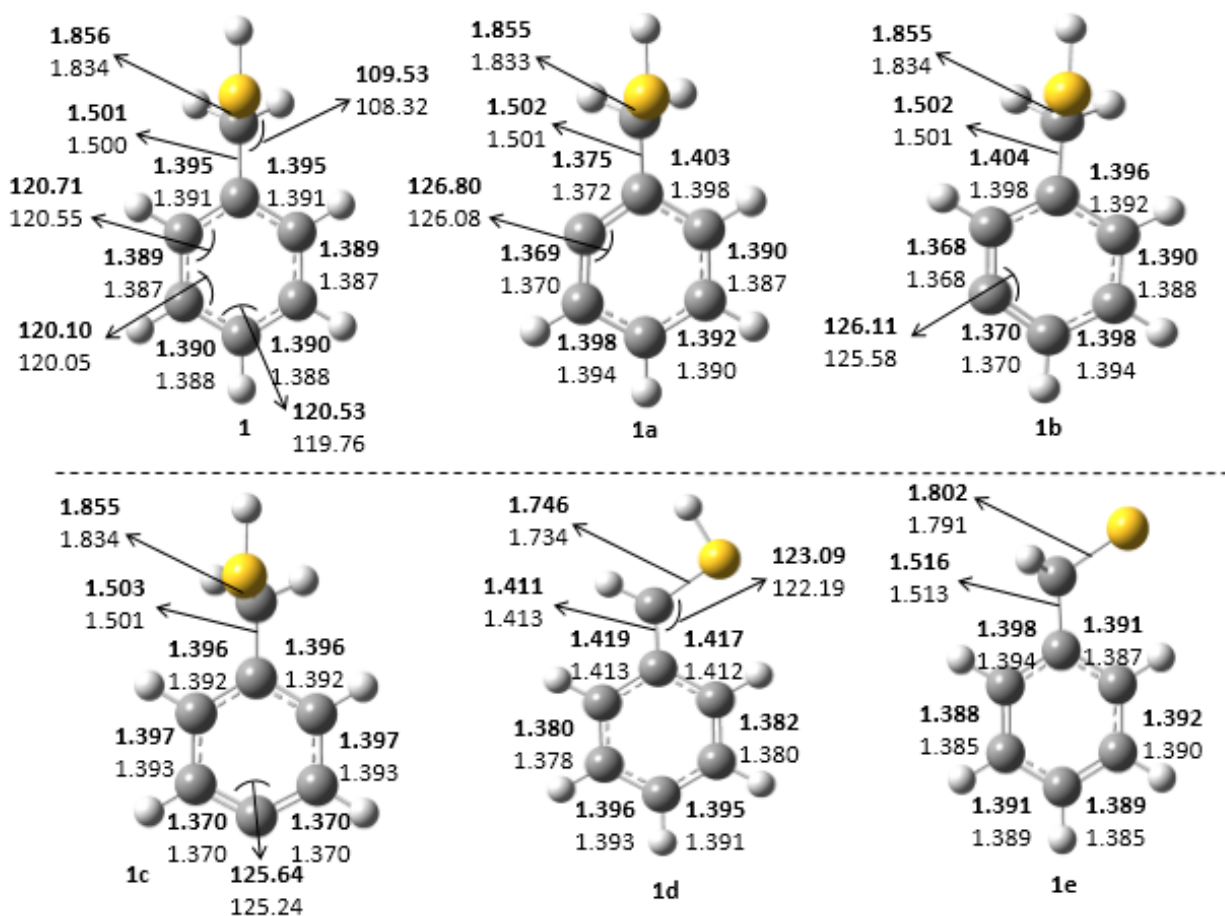


**Figure 2.1b.** Geometrical parameters (bond angle in degrees and bond distances in Å) of benzylmercaptan (**2**), and all different possible radical isomers (**2a**, **2b**, **2c**, **2d** and **2e**). Bold: (U)B3LYP/cc-pVTZ, Normal: (U)M06-2X/cc-PVTZ levels of theory.

While there was an increase in the bond angle, a decrease in bond length value was observed adjacent to the radical center compared to that of the parent molecule. Consequently, there was an increase in bond length values alternate to the radical center when compared to the parent molecule. Other bond lengths did not have any significant change. The results were consistent at both levels of theory.

### 2.1.3 Relative Stability Based on Absolute Energy

In order to understand the relative stability of the radical isomers of benzylalcohol and benzylmercaptan, their absolute energy from frequency calculations were compared. On comparison **1d** was found to be most stable followed by **1e**, **1b**, **1c** and then **1a**, for benzylalcohol.

Similar results were observed for benzylmercaptan radical isomers too. Slight variation in the values was observed at different level of theory. The results are tabulated (**Table 2.1a,b**).

**Table 2.1a:** Relative energies (kcal/mol) of dehydrobenzylalcohol isomeric radicals at (U)B3LYP/cc-pVTZ, (U)M06-2X/cc-pVTZ and CBS-QB3 level of theory.

Levels of Theory	1a	1b	1c	1d	1e
(U)B3LYP/cc-pVTZ	32.0	31.3	31.8	0.0	19.6
(U)M06-2X/cc-pVTZ	28.8	28.3	28.8	0.0	20.7
CBS-QB3	36.5	35.4	35.9	0.0	21.4

**Table 2.1b:** Relative energies (kcal/mol) of dehydrobenzylmercaptan isomeric radicals at (U)B3LYP/cc-pVTZ, (U)M06-2X/cc-pVTZ and CBS-QB3 level of theory.

Levels of Theory	2a	2b	2c	2d	2e
(U)B3LYP/cc-pVTZ	30.5	30.4	30.8	0.0	4.4
(U)M06-2X/cc-pVTZ	27.9	27.5	27.4	0.0	1.7
CBS-QB3	31.5	31.1	31.4	0.0	22.6

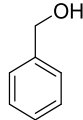
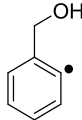
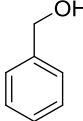
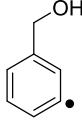
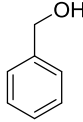
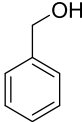
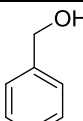
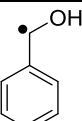
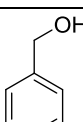
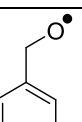
#### 2.1.4 Relative Stability Based on Bond Dissociation Energy (BDE)

Bond dissociation energy (BDE) for a given bond in a molecule can be measured as the difference in enthalpies of related to the products (arising due to homolytic cleavage) and reactants involved in the reaction. In this regard, BDEs of benzylalcohol and benzylmercaptan have been estimated that can lead to all the individual dehydro-radical isomers (**Table 2.2a,b**). Particularly, the difference in energies of products and reactants are computed for the first homolysis of various C-H, O-H, and S-H bonds such that the target radical isomers are generated.

Change in enthalpy of this reaction can provide information about the relative stability pattern of the radical isomers. BDE is inversely related to the stability of the radical. Radical having a high value of BDE value will mean higher amount of energy taken to form that radical, which implies that the corresponding radical will be less stable. We found the order of relative stability

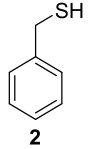
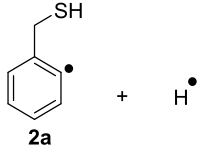
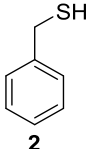
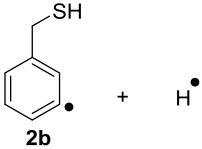
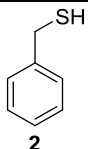
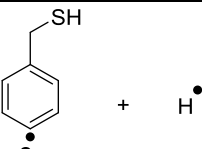
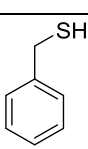
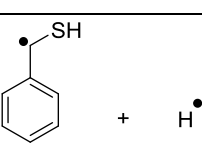
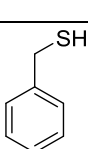
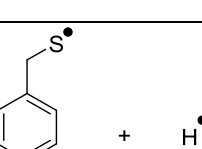
to be **1d** > **1e** > **1b** > **1c** > **1a**. The results are consistent with the trend observed for relative stability. Similar trends were noticed in the case of benzylmercaptan too.

**Table 2.2(a)** Bond Dissociation Energies (BDEs) of first homolytic C-H bond (in kcal/mol) of dehydrobenzylalcohol radical isomers.

Reactant	Products	BDE <sup>a</sup> (kcal/mol)
 <b>1</b>	 + H• <b>1a</b>	<b>110.5</b> <i>111.6</i> 116.3
 <b>1</b>	 + H• <b>1b</b>	<b>110.5</b> <i>111.0</i> 115.3
 <b>1</b>	 + H• <b>1c</b>	<b>111.0</b> <i>111.4</i> 115.7
 <b>1</b>	 + H• <b>1d</b>	<b>79.2</b> <i>82.7</i> 84.3
 <b>1</b>	 + H• <b>1e</b>	<b>98.7</b> <i>103.2</i> 105.7

<sup>a</sup>Bold font: (U)B3LYP/cc-pVTZ, Italics font: (U)M06-2X/cc-pVTZ, Normal font: CBS-QB3 level of theory

**Table 2.2(b)** Bond Dissociation Energies (BDEs) of first homolytic C-H bond (in kcal/mol) of dehydrobenzylmercaptan radical isomers.

Reactant	Products	BDE <sup>a</sup> (kcal/mol)
		<b>110.8</b> <i>111.6</i> 115.9
		<b>110.7</b> <i>111.2</i> 115.6
		<b>111.0</b> <i>110.8</i> 115.8
		<b>80.2</b> 83.6 84.5
		<b>83.8</b> <i>84.7</i> 106.2

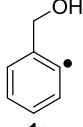
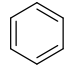
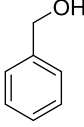
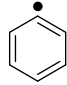
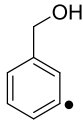
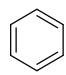
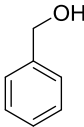
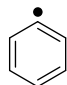
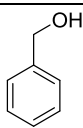
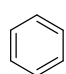
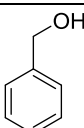
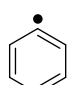
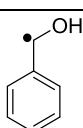
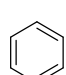
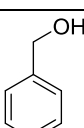
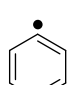
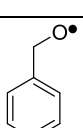
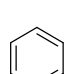
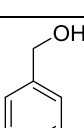
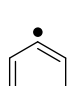
<sup>a</sup>Bold font: (U)B3LYP/cc-pVTZ, Italics font: (U)M06-2X/cc-pVTZ, Normal font: CBS-QB3 level of theory.

### 2.1.5 Relative Stability Based on Radical Stabilization Energy (RSE)

Isodesmic reaction is a class of chemical reaction used as a hypothetical reaction in thermochemistry, in which similar types of bonds are broken in the reactant and formed in the product. The change in the enthalpy of such reaction is defined and estimated to be the radical stabilization energy (RSE) of the radical. The numerical values associated with RSE of similar reactions or analogous radicals can be used as a quantitative tool and comparison of the stability in organic molecules. In this regard, we have chosen benzene as the common reactant for all isodesmic reactions (as shown in **Table 2.3a,b**). A more positive value of RSE will imply that radical to be more stable in comparison to other radicals as a positive value will mean the reaction

to move in the forward direction in favor of the product (which in our case is radical). From the calculated RSEs values, it is observed that **1d** is the most stable radical as it has the highest positive value out of all five radical isomers. Based on the RSEs value, the order of relative stability was found out to be **1d** > **1e** > **1b** > **1c** > **1a**, which confirms the order we got from the BDE and relative energy calculations. The order of relative stability of benzylmercaptan was found to be consistent with the order we found for benzylalcohol.

**Table 2.3a:** Radical stabilization energies (RSEs) (in kcal/mol) of dehydrobenzylalcohol isomeric radicals calculated using isodesmic reaction.

Reactant	Products	RSE <sup>a</sup> (kcal/mol)
 <b>1a</b> + 	 <b>1</b> +  <b>5</b>	<b>0.1</b> <i>-0.5</i> <i>-0.9</i>
 <b>1b</b> + 	 <b>1</b> +  <b>5</b>	<b>0.2</b> <i>0.2</i> <i>0.2</i>
 <b>1c</b> + 	 <b>1</b> +  <b>5</b>	<b>-0.3</b> <i>-0.3</i> <i>-0.3</i>
 <b>1d</b> + 	 <b>1</b> +  <b>5</b>	<b>31.5</b> <i>28.4</i> <i>31.1</i>
 <b>1e</b> + 	 <b>1</b> +  <b>5</b>	<b>12.0</b> <i>7.9</i> <i>9.9</i>

<sup>a</sup>Bold font: (U)B3LYP/cc-pVTZ, Italics font: (U)M06-2X/cc-pVTZ, Normal font: CBS-QB3 level of theory.

**Table 2.3b:** Radical stabilization energies (RSEs) (in kcal/mol) of dehydrobenzylmercaptan isomeric radicals calculated using isodesmic reaction.

Reactant	Products	RSE <sup>a</sup> (kcal/mol)
 2a	 2         + 5	<b>-0.2</b> <i>-0.5</i>
 2b	 2         + 5	<b>-0.1</b> <i>-0.1</i>
 2c	 2         + 5	<b>-0.4</b> <i>0.3</i>
 2d	 2         + 5	<b>30.4</b> <i>27.5</i>
 2e	 2         + 5	<b>26.8</b> <i>26.4</i>

<sup>a</sup>Bold font: (U)B3LYP/cc-pVTZ, Italics font: (U)M06-2X/cc-pVTZ

### 2.1.6 Spin Density and Molecular Orbitals

Electron density is a measure of the probability of an electron being at a particular position, and it is proportional to the square of the wave function. Now, spin density is electron density defined for the open-shell system. It is a measure of the localization/delocalization of the free radical on a specific atom in an open-shell system. It is calculated using the difference in the magnitude of electrons in  $\alpha$  and  $\beta$  spin on a particular atom. In general, for an open-shell system (with one unpaired electron) value of total spin density is equal to one, if that electron is localized on that particular atom. The value could differ from one if the electron is delocalized. Spin density is mainly used in combination with singly occupied molecular orbitals (SOMO) to describe the nature of radical, i.e.,  $\sigma$ - or  $\pi$ - type based on which the electron occupies its space.

The value of spin density in **1a**, **1b**, and **1c** are ranging from 0.92 to 1.06 at (U)B3LYP/cc-pVTZ and (U)M06-2X/cc-pVTZ implying that the radical is localized mostly over the radical center and SOMO images show that the radical is  $\sigma$ - type (**Figure 2.2**). Spin density values for **1d** was not close to one, implying that the radical is delocalized, which was strengthened by the fact that the value of spin density shown by the carbon atoms on the ring was not close to zero. SOMO images show that the electrons were  $\pi$ - type in nature. In the case of **1e**, the value was close to one, but still, there was some delocalization, which could be seen by the  $\pi$ - nature using SOMO images.

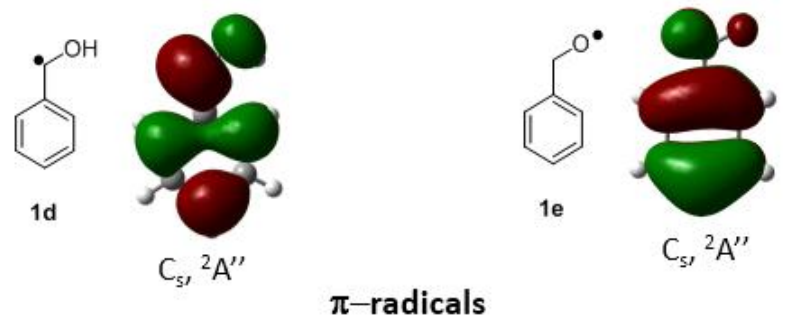
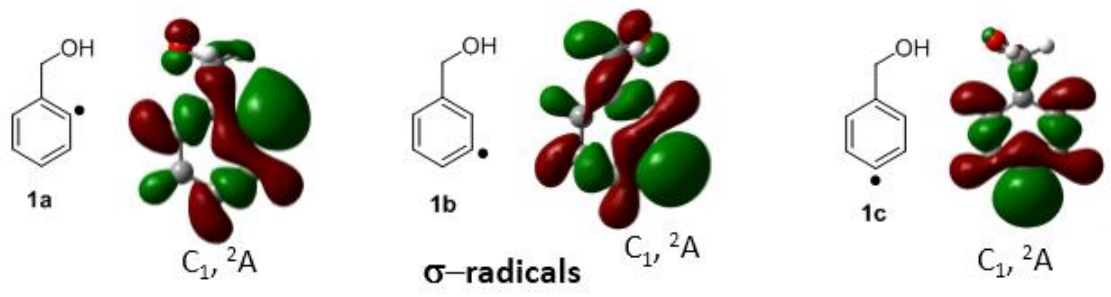
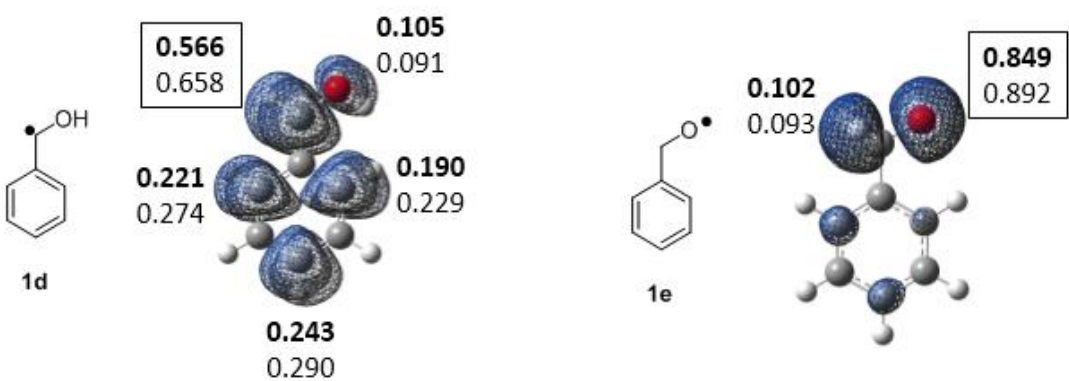
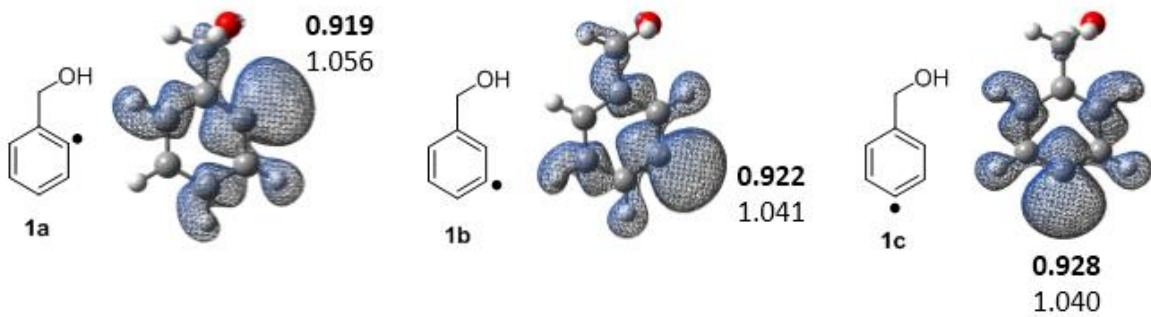


**Figure 2.2a.** Spin density values at (U)B3LYP/cc-pVTZ (bold), (U)M06-2X/cc-PVTZ levels of theory, and molecular orbitals corresponding to SOMO for the dehydrobenzylalcohol radical isomers (level of theory and the molecular orbitals are rendered at an isovalue 0.05).



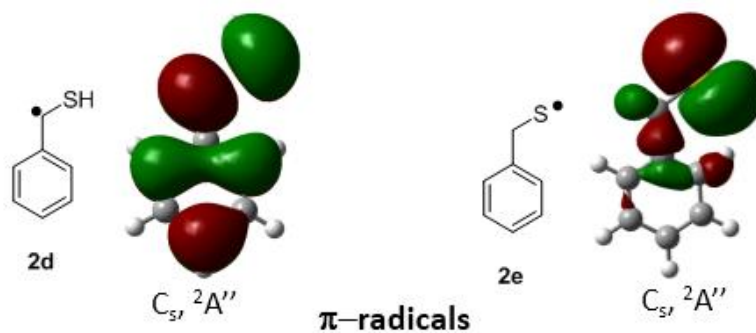
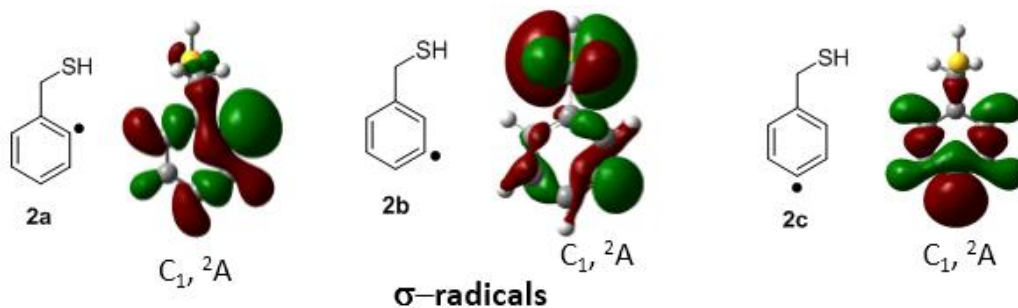
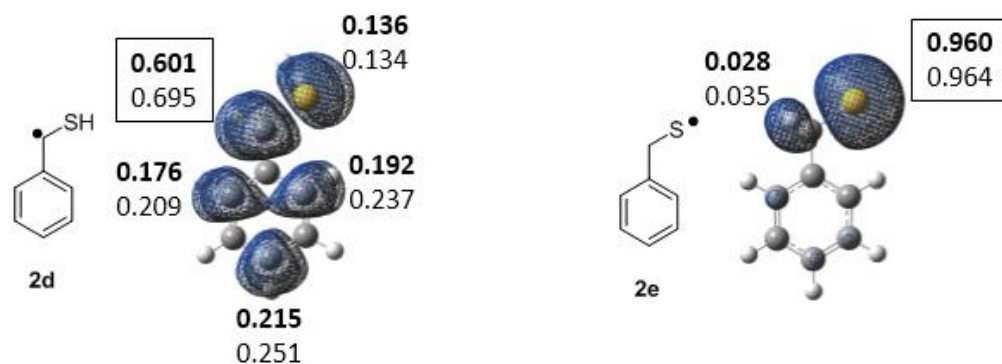
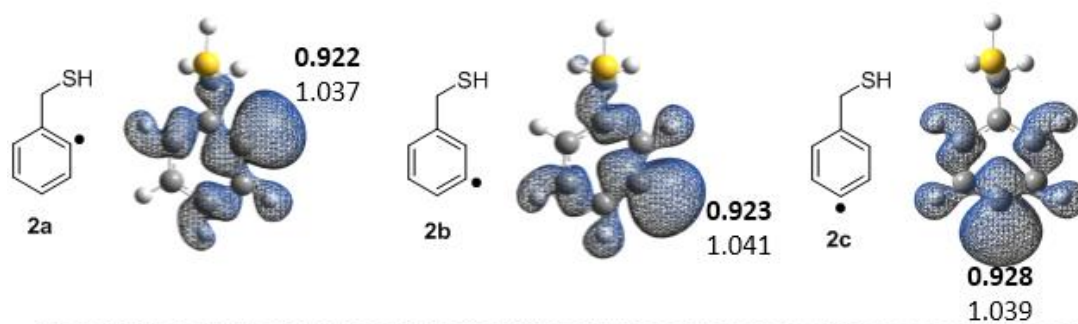


**Figure 2.2b.** Spin density values at (U)B3LYP/cc-pVTZ (bold), (U)M06-2X/cc-pVTZ levels of theory, and molecular orbitals corresponding to SOMO for the dehydrobenzylmercaptan radical isomers (level of theory and the molecular orbitals are rendered at an isovalue 0.05).

### 2.1.7 Thermal Reactivity Studies

In this section, we have discussed in details the reactivity studies of the target radicals in thermal gas phase conditions to understand the kinetic stability. Thermal reactivity studies have been carried out only for the ground electronic states of the concerning radicals, whereas photochemical reactivity studies include absorption of a photon from the light in the ground state to the attainment of electronically excited states have not been considered. All the reactants, products, transition states, and reactive intermediates are optimized to the lowest energy ground states. However, many of the products under photochemical channels can be the same as in the thermal reaction channels, and so the species can be used for understanding the potential products in the case of experiments.

In this respect, different channels are considered on ground state thermal reactivity to gain information about the lowest energy pathway of radical isomers of benzylalcohol and benzylmercaptan as follows:

- i) 1,2-, 1,3- and 1,4-H shift in the interconversions between *o*-, *m*-, and *p*- isomers
- ii) Unimolecular decomposition pathways

Geometry optimizations and frequency calculations in this respect have been performed at (U)B3LYP/cc-pVTZ and (U)M06-2X/cc-pVTZ levels of theory.

#### 2.1.7.1 1,2-, 1,3- and 1,4-Hydrogen Shift

H-shift is a type of sigmatropic rearrangement in which a hydrogen atom migrates to a new spot, which in the case of 1,2 H-shift is one atom away from its starting point, with a simultaneous shift of a  $\pi$ -bond. Many types of H-shifts are possible, out of which we have worked on 1,2-, 1,3- and 1,4-H-shifts. The most straightforward pathway for H-shift is the 1,2 H-shift, which is the interconversion of *ortho*- to *meta*- and then *meta*- to *para*- in the phenyl radicals. All reactants, products, and transition states were optimized in case of *ortho*-, *meta*- and *para*- isomers of benzylalcohol and benzylmercaptan. Potential energy surface for *ortho*-, *meta*- and *para*- isomers are shown in **figure 2.3a,b**. Activation barriers were calculated using the difference between the zero-point energies of reactants and transition states. We found out that the energy barriers corresponding to 1,2 H-shifts were in the realm of 60 kcal/mol. Furthermore, 1,3- and 1,4-H-shifts seem to be low energy pathways, considering their activation energy barrier, which were in the

order of 34.8 and 14.0 kcal/mol (for benzyl alcohol radicals) and 35.8 and 2.7 kcal/mol (for benzylmercaptan radicals).

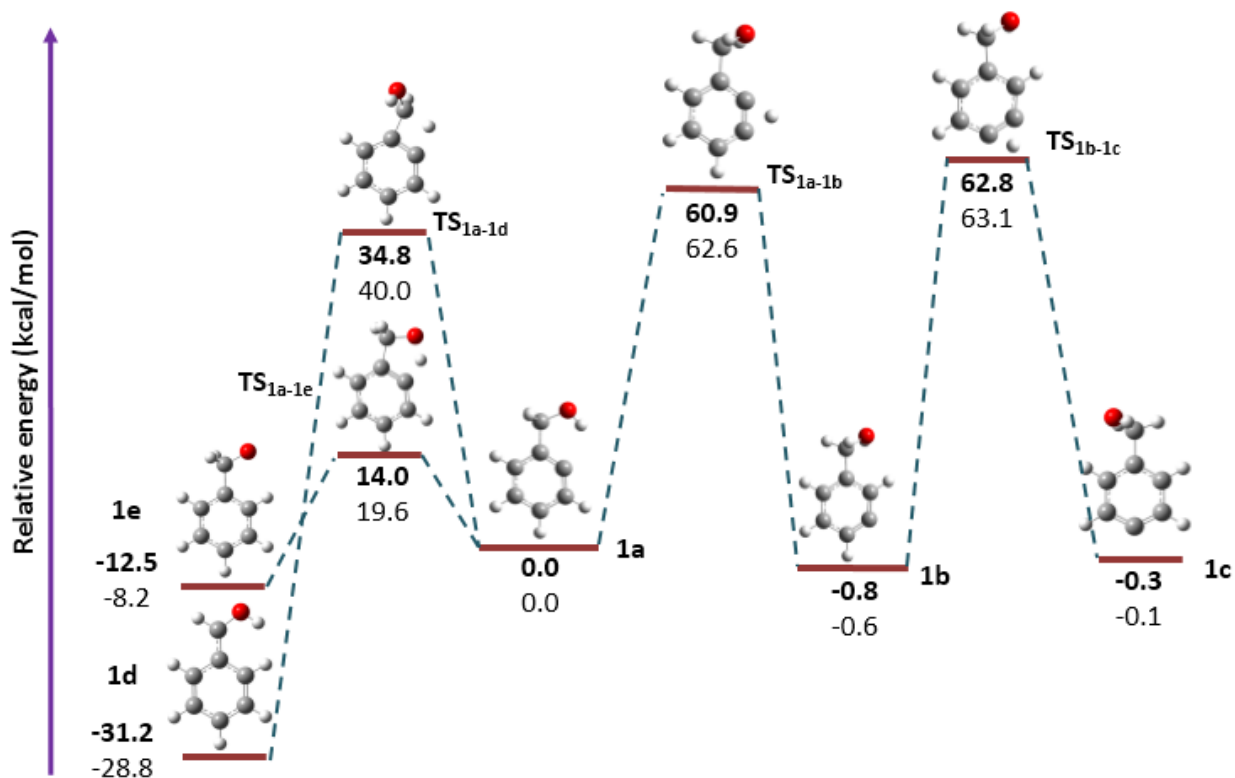


**Figure 2.3a:** Potential energy diagrams corresponding to the 1,2-, 1,3- and 1,4-H-shifts in **1a**, **1b**, **1c**, **1d** and **1e** (reactant, corresponding TS and corresponding product) calculated at (U)B3LYP/cc-pVTZ (bold) and (U)M062X/cc-pVTZ (normal font) levels of theory.

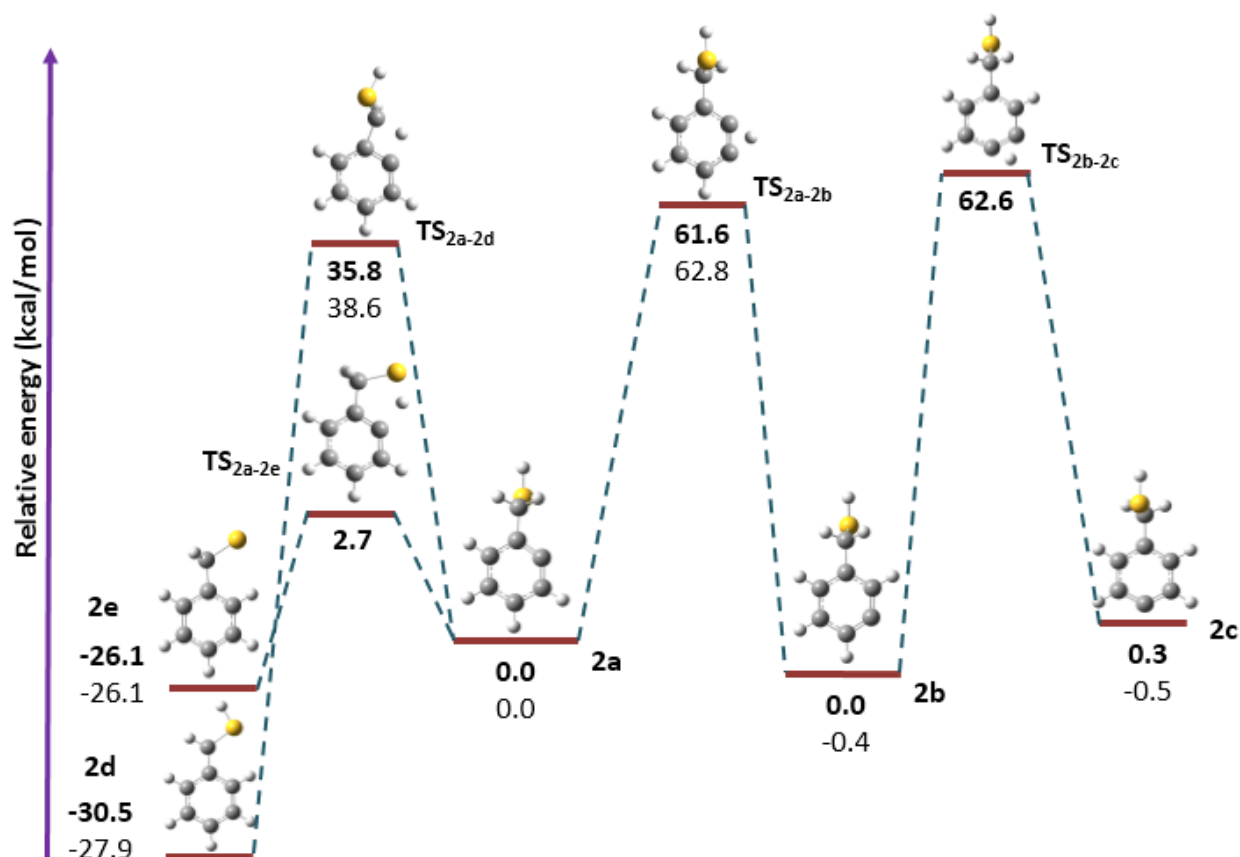


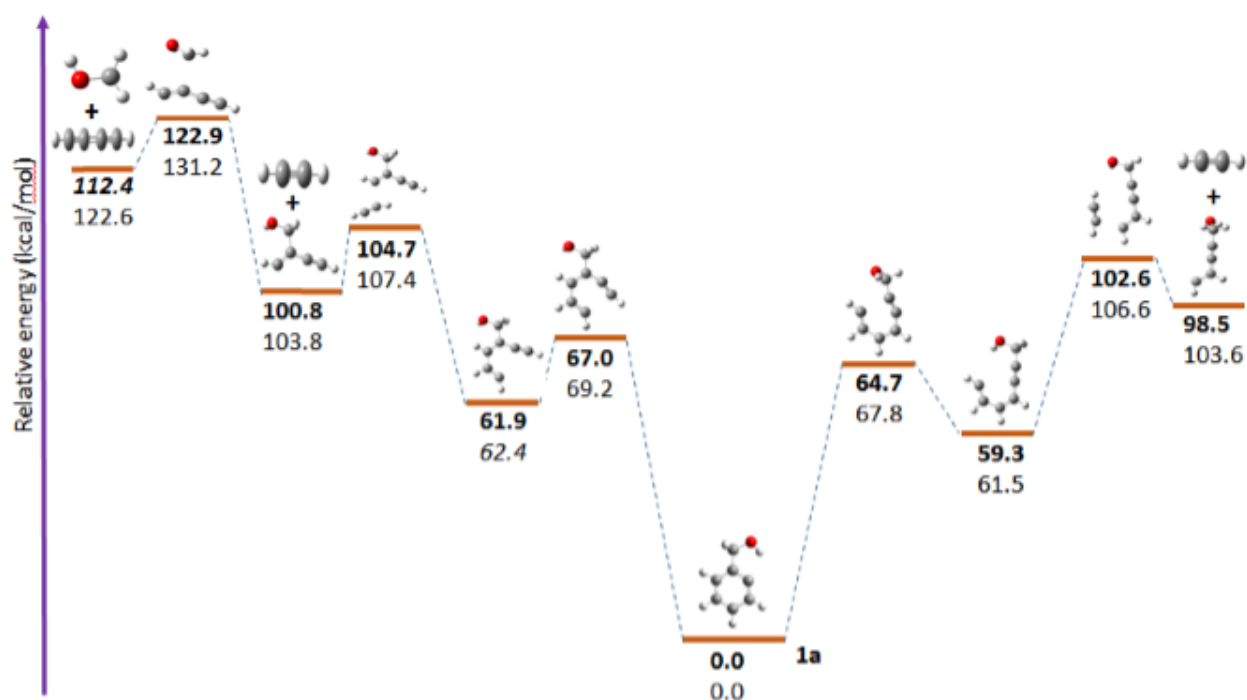
**Figure 2.3(b):** Potential energy diagrams corresponding to the 1,2-, 1,3- and 1,4-H shifts in **2a**, **2b**, **2c**, **2d** and **2e** (reactant, corresponding TS and corresponding product) calculated at (U)B3LYP/cc-pVTZ (bold) and (U)M062X/cc-pVTZ (normal font) levels of theory.

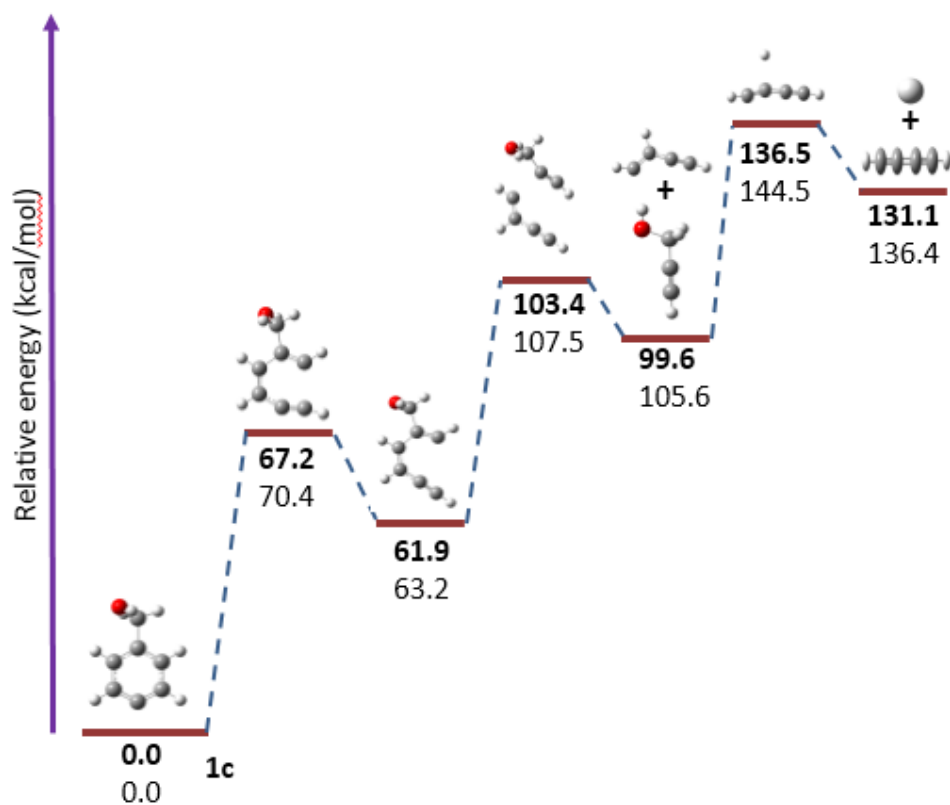
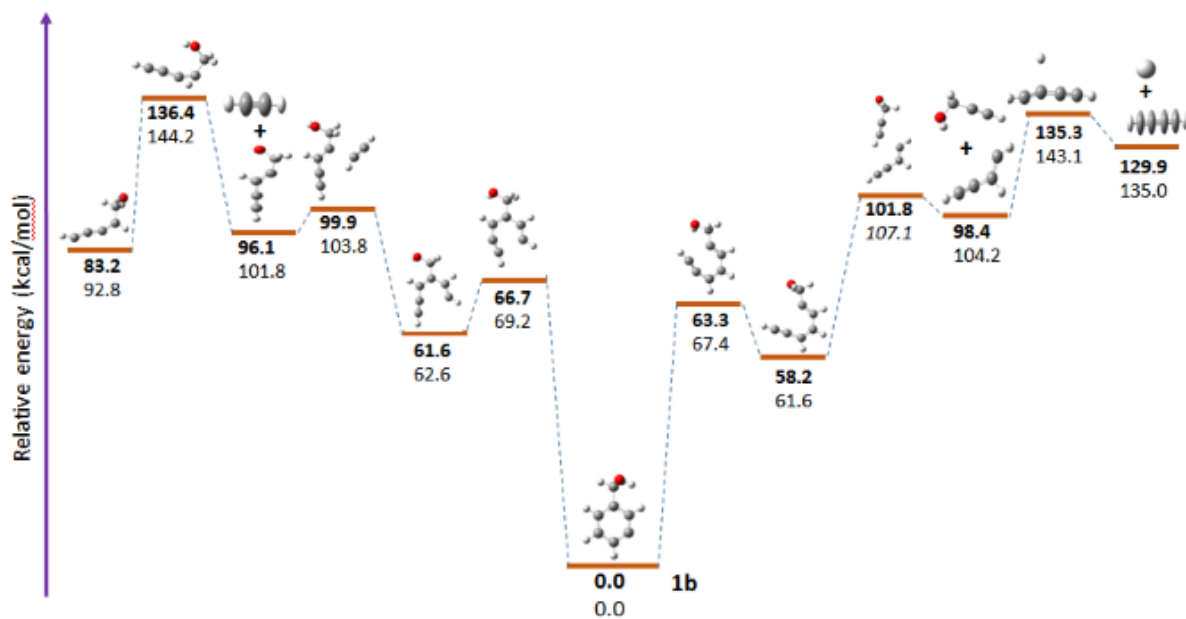
From **figure 2.3a** and **figure 2.3b**, it can be quickly figured out that the product corresponding to 1,4-H shift is kinetically more favored as the barrier is lowest in this case even though the product corresponding to 1,3-H shift is thermodynamically more favored. Activation energy barriers for 1,2- and 1,3-H shifts were more or less similar in all the cases, but 1,4 shifts had different barriers, which could be because of the different sizes of heteroatom. 1,4 shift was only possible in the case of *ortho*- isomer and not in other isomers because of geometrical constraints.

### 2.1.7.2 Unimolecular Decomposition

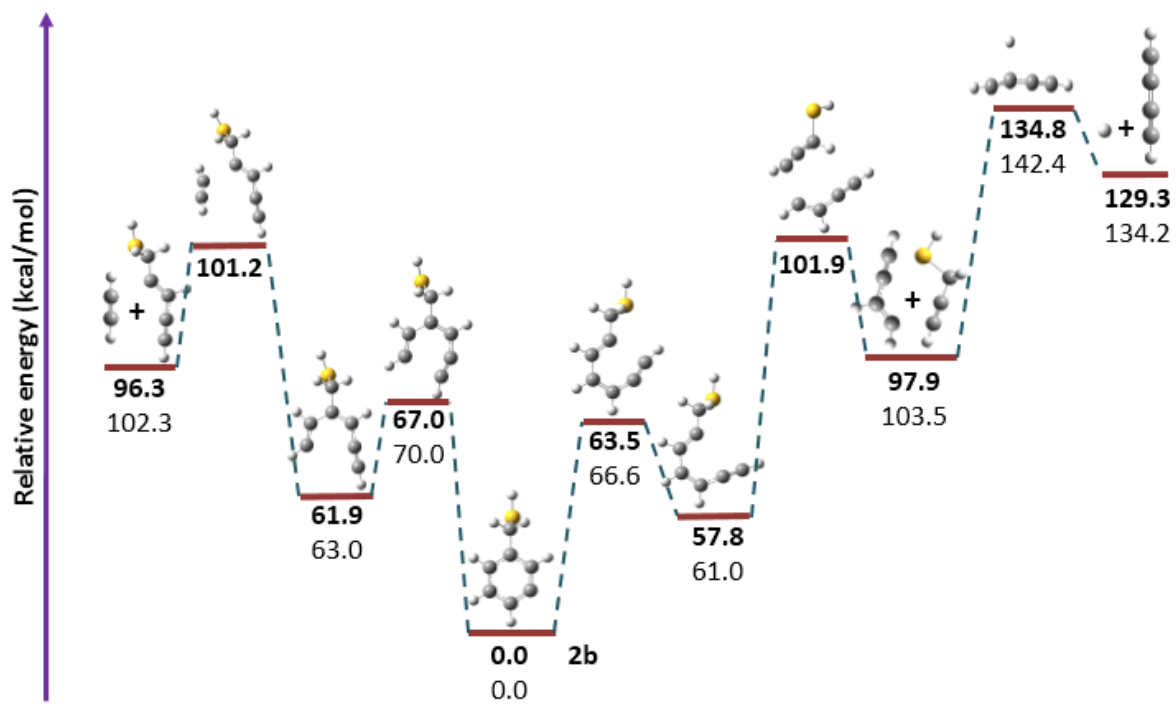
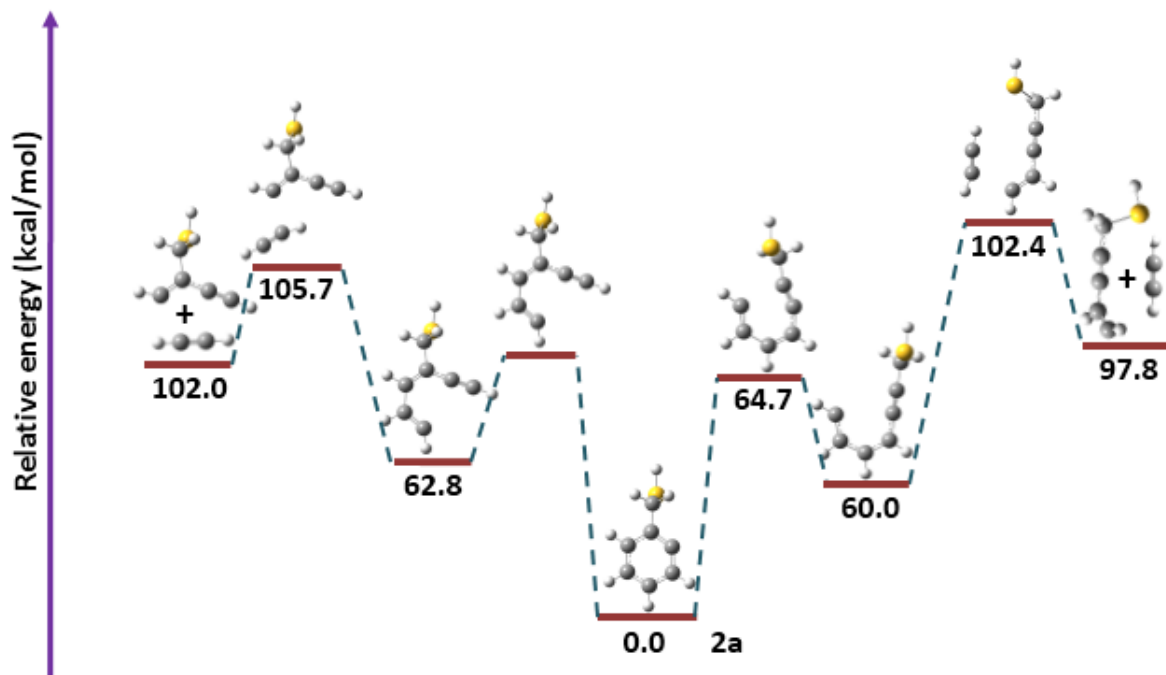
In this part of reactivity studies, we have done the computational studies on unimolecular decomposition channels for *ortho*-, *meta*-, and *para*- radical isomers. These are gas-phase reactions but give us insight about possible photoproducts, which could be detected experimentally. In this regard, these pathways have led to ring opening and fragmentation pathways to provide final

products. **Figure 2.4a,b** suggests that the ring opening is a very high energy-demanding step. Bond lengths of C-C play a crucial role in determining the energy barrier for the TS in every step. The carbon on which the radicals are forming in *ortho*-, *meta*-, and *para*- have smaller C-C adjacent bond lengths and longer C-C alternate bond lengths in comparison to the parent molecule. So, it is very much possible for the alternate C-C bond lengths to break in case irradiation is done with light of appropriate wavelength. The increase in the alternative C-C bond length in comparison to the parent molecule was considered for predicting the ring-opening channel through the cleavage of that particular bond





**Figure 2.4a:** Potential energy diagrams corresponding to the ring-opening and fragmentation of **1a**, **1b**, and **1c** (reactant, corresponding TS and corresponding product) calculated at (U)B3LYP/cc-pVTZ (bold) (U)M062X/cc-pVTZ (normal font) levels of theory.



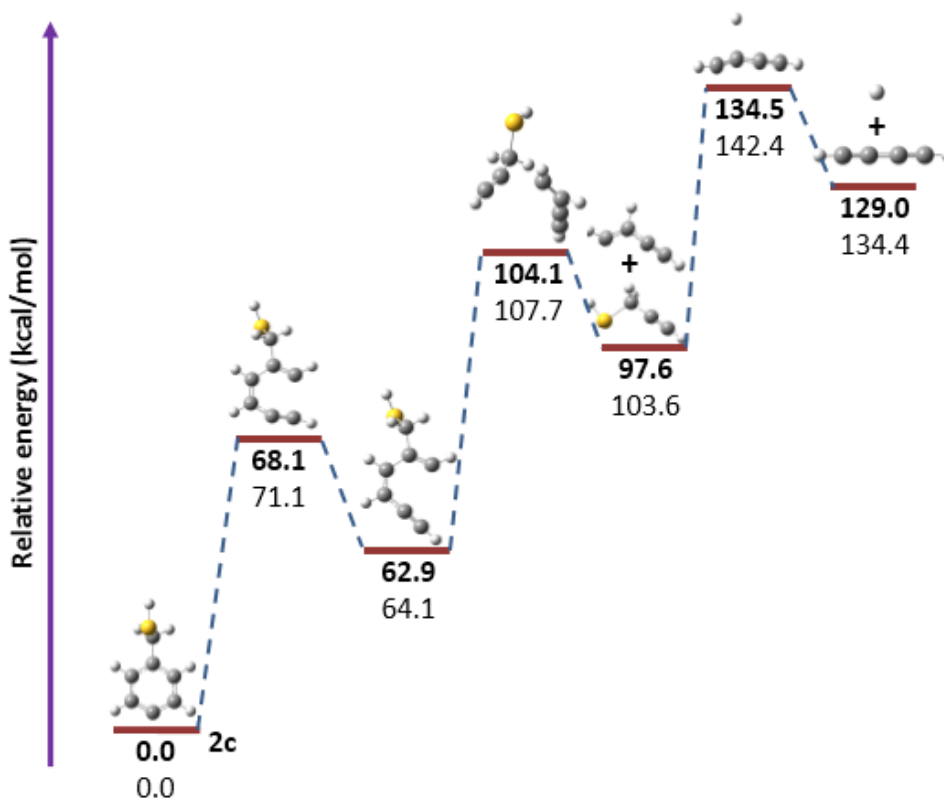


**Figure 2.4b:** Potential energy diagrams corresponding to the ring fragmentation of **2a**, **2b**, and **2c** (reactant, corresponding TS and corresponding product) calculated at (U)B3LYP/cc-pVTZ (bold) and (U)M062X/cc-pVTZ (normal font) levels of theory.

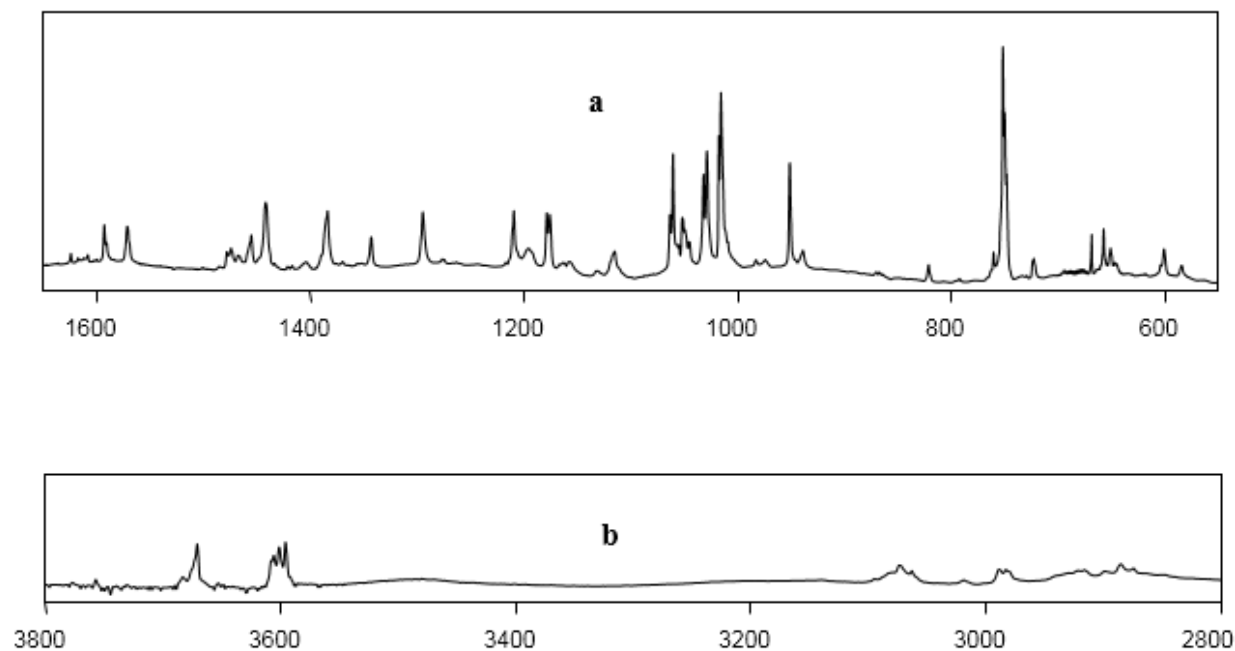
From **figure 2.4a** and **2.4b**, we have concluded that two possible ring opening channels each are possible in the case of benzylalcohol and benzylmercaptan (*ortho*-, *meta*-, and *para*-). For *ortho*- and *meta*- radical isomers, two pathways were observed, as both of the radicals are unsymmetrical. For *para*- isomer, there was only one pathway possible as the radical was symmetrical. These products were computed for the thermal unimolecular decomposition channels at their respective ground states. For the formation of photoproducts, firstly the molecule has to be excited using light of appropriate wavelength. However, many of these products can also be potential photoproducts under irradiation with light of appropriate wavelength.

## 2.2 Matrix Isolation Infrared Spectroscopic and Computational Studies on 2-Iodobenzylalcohol



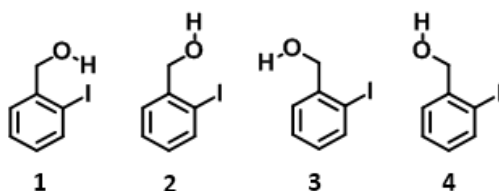
After the completion of computational studies of all possible radical isomers of benzylalcohol and benzylmercaptan, we shifted our interests on matrix isolation experiments. One of the main objectives of this study was to see the photochemistry of matrix isolated 2-iodobenzylalcohol with the use of infrared spectroscopy as a tool. This technique is particularly well suited for the detection of reactive intermediates like radicals, carbenes, nitrenes, etc. which has a very short lifetime at room temperature and ambient pressure. In this technique, reactive intermediates are generated and trapped in its natural form under very low temperature and high vacuum. In these experiments, an inert gas is taken as the host matrix gas (usually in a high concentration) so that the radicals do not interact with each other and well-resolved spectra is obtained.

In this regard, 2-iodobenzylalcohol was co-deposited with an excess of argon gas for 2 hours and 30 minutes at 70°C onto a cold KBr window under cryogenic conditions (4 K). IR spectrum of 2-iodobenzylalcohol in matrix-isolated conditions is shown in **figure 2.5**.



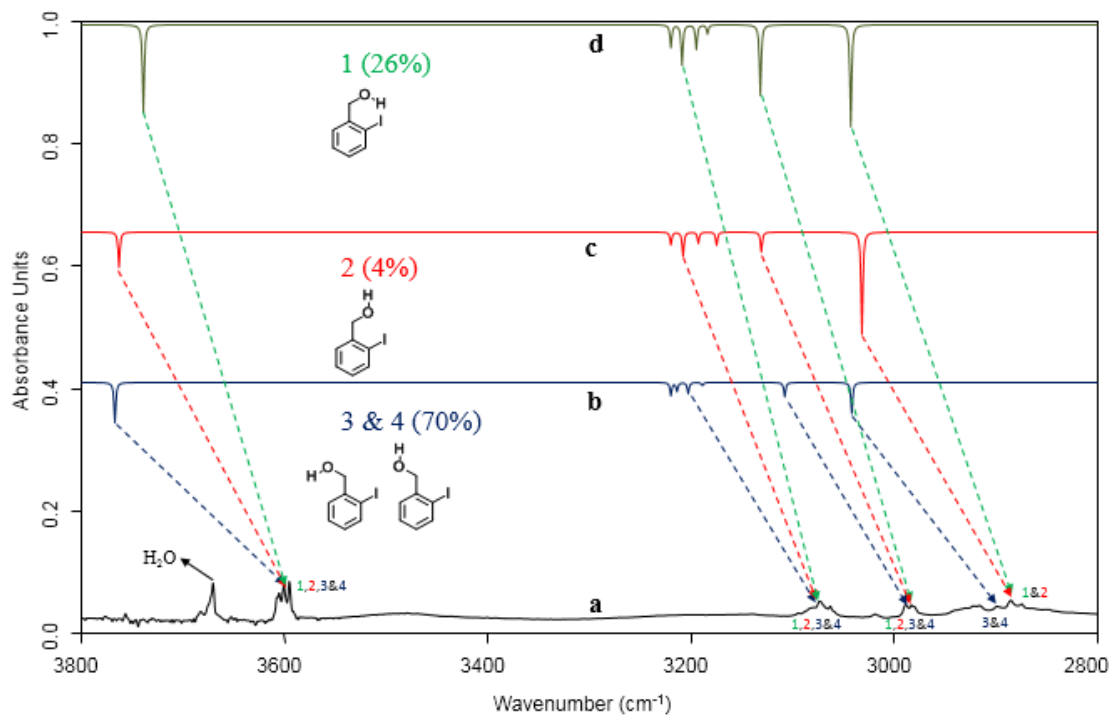
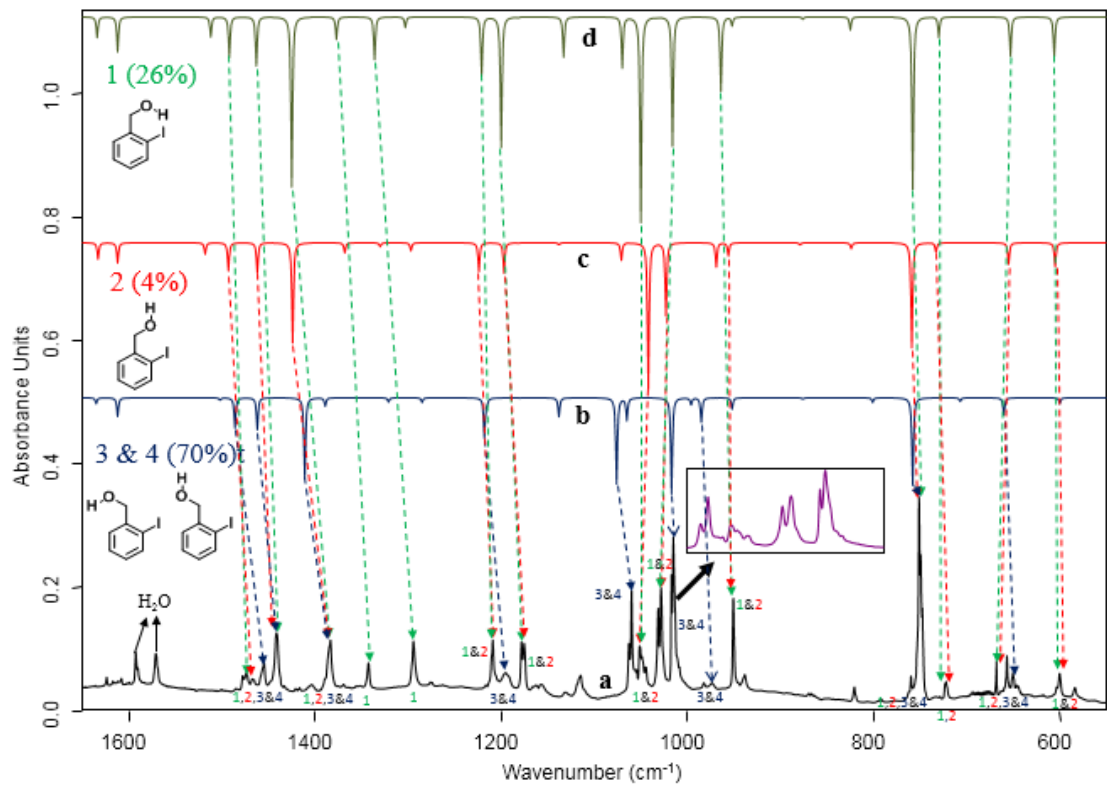
**Figure 2.5:** Deposition spectra of 2-iodobenzylalcohol in argon matrix at 4 K (region wise): (a) 1650 – 550  $\text{cm}^{-1}$ ; & (b) 3800 – 2800  $\text{cm}^{-1}$ .

Usually, sharp signals are the general feature of matrix isolated IR spectrum for any precursor molecule with a peak width at half maxima of around  $1\text{ cm}^{-1}$ , but in our case, we saw relatively broad signals. These broad signals are supposed to be because of the different spatial orientations of O-H moiety attached directly to the methyl group in 2-iodobenzylalcohol. These broadening in the peaks arising due to the conformations can be a plausible reason. In the case of 2-iodobenzylalcohol, there are four major conformers possible, namely, **1**, **2**, **3**, and **4** (shown in **figure 2.6**). Computational studies have been performed on these four conformers at the B3LYP/DGTZVP level of theory, and we observed that conformer **3** and **4** were degenerate and the most stable, followed by **1** and then **2**.



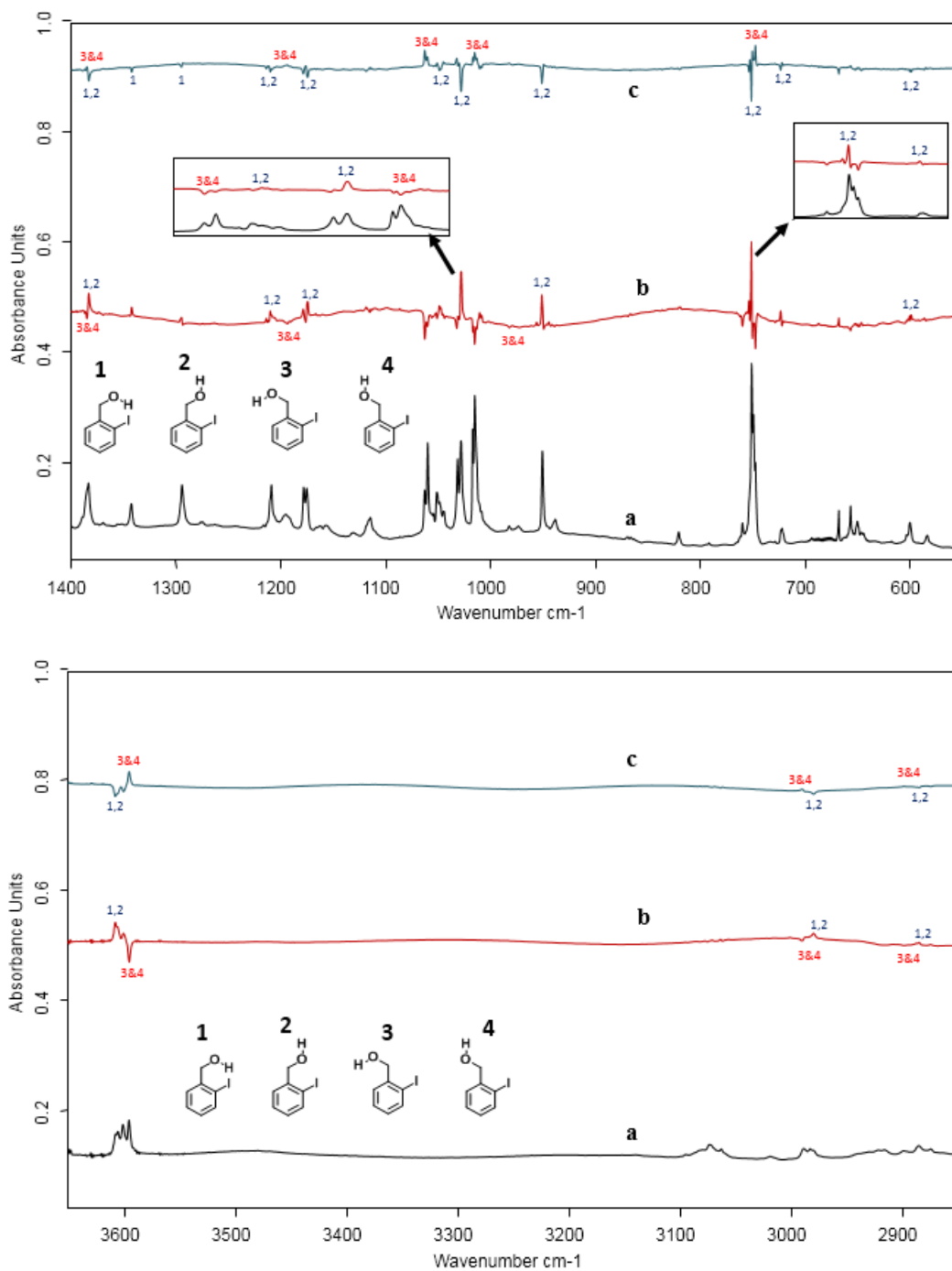
**Figure 2.6:** Major conformers of 2-iodobenzylalcohol

The computed spectra for conformer **3** and **4** were the same as they were degenerate. By comparing the computed spectrum and the deposition spectrum of 2-iodobenzylalcohol, we can safely say that the deposition spectrum has all the possible conformations as shown in **figure 2.7**.



**Figure 2.7:** (a) Deposition spectrum of 2-iodobenzylalcohol in argon matrix at 4 K (region wise): (top) 1650 – 550  $\text{cm}^{-1}$ ; & (bottom) 3800 – 2800  $\text{cm}^{-1}$ ; (b, c & d) Calculated spectrum of conformers **1**, **2**, **3** and **4**, respectively (B3LYP/DGTZVP, unscaled).

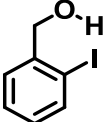
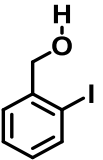
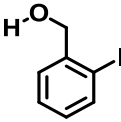
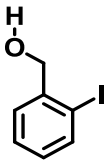
After the deposition of 2-iodobenzylalcohol over the KBr window at 4 K, we irradiated the deposited precursor molecule with 365 nm light. Upon irradiation with 365 nm, we observed the decrease in the intensity of some signals with a simultaneous increase in other features. These changes in signals indicate conformational changes due to light rather than the formation of new photoproducts (which was the expected result). Irradiation at 254 nm after the irradiation at 365 nm shows the reversal of changes i.e., the signal intensities changes. The signals that were decreased initially after irradiation at 365 nm were now increased with 254 nm light and vice-versa.



**Figure 2.8:** (a) Deposition spectrum of 2-iodobenzylalcohol in argon matrix at 4 K (region wise): (top) 1650 – 550 cm<sup>-1</sup>; & (bottom) 3800 – 2800 cm<sup>-1</sup>; (b) Difference spectrum after irradiation at 365 nm (c) Difference spectrum after irradiation at 254 nm (signals pointing upward direction signifies the formation of new species and those pointing downward disappear upon irradiation).

Energy calculations were done for all four conformers of 2-iodobenzylalcohol to check the relative stability order of these conformers at different levels of theory. It was concluded that conformers **3** and **4** were degenerate in energy and the most stable ones followed closely by conformer **1**. Conformer **2** was found to be the least stable of the possible conformers. Their Boltzmann populations have been estimated using the formula  $N_2/N_1 = \exp(-\Delta E/k_bT)$  using the zero point corrected electronic energy. Relative energies and relative Boltzmann populations (in the parenthesis) are shown in **Table 2.4**.

**Table 2.4:** Relative energy and relative Boltzmann populations (in the parenthesis) of possible conformers of 2-iodobenzylalcohol at different level of theory.

Levels of theory	Conformers			
	 <b>1</b>	 <b>2</b>	 <b>3</b>	 <b>4</b>
<b>B3LYP/cc-pVTZ</b>	0.2 (26%)	1.3 (4%)	0.0 (35%)	0.0 (35%)
<b>M062X/cc-pVTZ</b>	0.3 (22%)	1.4 (4%)	0.0 (37%)	0.0 (37%)
<b>CCSD(T)/cc-pVTZ//B3LYP/cc-pVTZ</b>	0.0 (31.3%)	1.0 (6%)	0.0 (31.3%)	0.0 (31.3%)

All energies are in kcal/mol

Conformational scans were also done for 2-iodobenzylalcohol by changing the dihedral angle of C-C-C-O and energy barriers were found for the interchanging of conformer **1** & **3**, and **2** & **4** at different levels of theory.

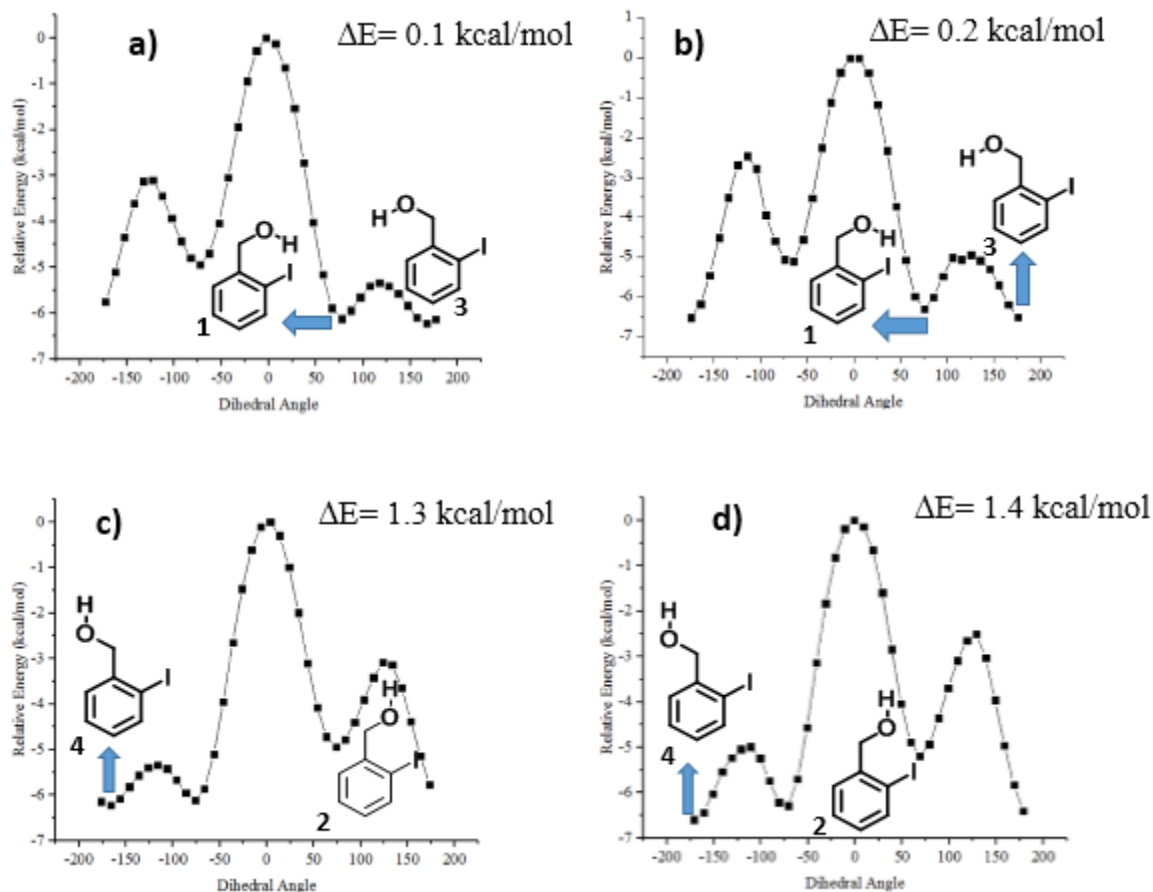


**Figure 2.9:** Potential energy surface (PES) scan for 2-iodobenzylalcohol upon changing the dihedral angle C-C-C-O. PES scan from Conformer **1** to Conformer **3** (a) at B3LYP/cc-pVTZ; (b) at M06-2X/cc-pVTZ; PES scan from Conformer **2** to Conformer **4** (c) at B3LYP/cc-pVTZ; (d) at M06-2X/cc-pVTZ.

Using **figure 2.9**, we were able to find the barriers for interconversions of the conformers (**1-3** and **2-4**) at different levels of theory. These barriers give us an idea of which light should be used so that light induced conformational changes are possible.

### 2.2.1 Possible Mechanisms for the light induced conformational changes

Based on the experimental data, we have clearly demonstrated that these conformational changes were observed upon irradiation at 365 nm. Interestingly, the conformational changes were reversed upon changing the wavelength from 365 nm to 254 nm. Such phenomena have been reported on 2-chlorobenzaldehyde by Nakata et al<sup>20</sup>. However, the conformational changes in 2-chlorobenzaldehyde is driven by the extended  $\pi$ -conjugation present in the carbonyl group. On the

other hand, the conformational changes in 2-iodobenzylalcohol is lacking such conjugation. In this regard, we propose the following two possible mechanisms:

- 1) Excited state conformational changes: Generally, after absorption of light, a molecule can be transferred from ground state to the electronically excited state. According to Franck-Condon principle, the transition between electronic states are possible given that the nuclear configurations are similar of the vibrational states. After the excitation to the excited state, molecule tends to relax to a minima and then comes back to the ground state. During the relaxation process, the molecule might have crossed a small barrier (relative to the ground state barrier for the interconversion) to attain a new conformation before returning back to the ground state potential energy surface (Figure 2.10a).
- 2) Hot ground state conformational changes: In an alternative mechanism, after attaining the excited state, the molecule tends to come back to the ground state. If the relaxation leads the molecule to reach higher vibrational state of the ground state potential energy surface, the molecule has excess energy to overcome the conformational barrier in such a way that it can undergo conformational changes (Figure 2.10b).

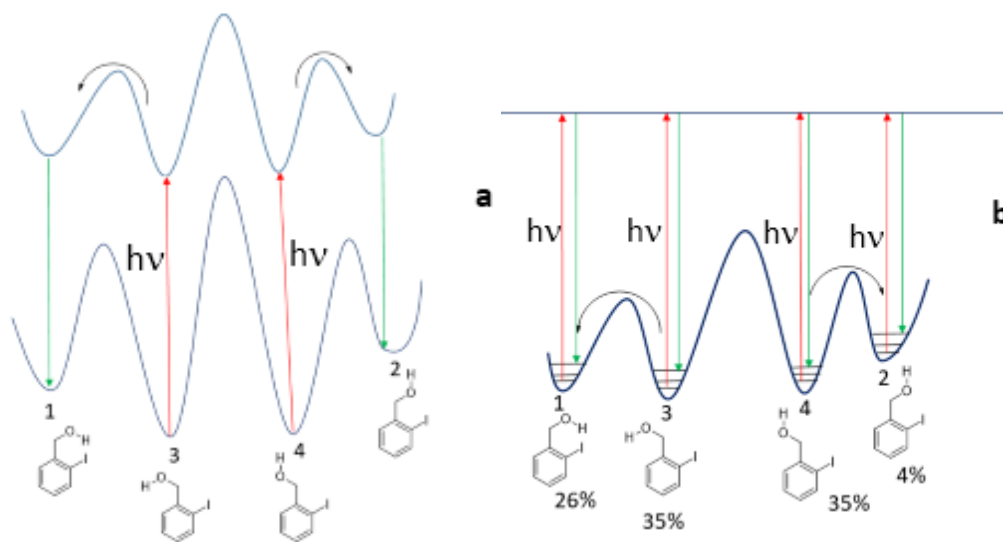


**Figure 2.10:** Two possible mechanisms for the light induced conformational changes in 2-iodobenzylalcohol (a) Excited state conformational changes; (b) Hot ground state conformational changes



In yet another view point, the presence of iodine (heavy atom) might be helpful in attaining the triplet excited state, and so the role of iodine in the light induced conformational changes cannot be ruled out. Further experimental and theoretical studies are needed to obtain a conclusion in this regard.

## Chapter 3. Conclusion and Perspectives

Computational investigations and matrix isolation spectroscopic studies are used to gain an insight into the photochemistry of 2-iodobenzylalcohol, which is the radical precursor used for the experiments. The computational studies were mainly concentrated on studying the possible radicals of benzylalcohol and benzylmercaptan using the electronic structure studies and reactivity pathways at different levels of theory. Using the results of electronic structure studies, we can now undoubtedly say that **1d** and **2d** were the most stable ones out of all the possible radical isomers. The stability was attributed to the delocalization of the radical with the benzene ring and  $p\pi$ - $p\pi$  or  $p\pi$ - $d\pi$  bonding characteristics. The next in the stability order was **1e** and **2e**, which were stable due to the delocalization over the heteroatom center. The phenyl radical analogues (**1a**, **1b**, **1c** or **2a**, **2b**, **2c**) were very close in energy, and their stability order was dependent on the level of theory used. Their instability is assigned to the localized nature of the radical. The localization and delocalization of the radical centers were studied using the spin density calculations and SOMO images.

Apart from these electronic structure studies, the kinetic stability of the radicals was examined using thermal reactivity studies. For this study, 1,2-H and 1,4-H shifts, along with unimolecular decomposition channels have been investigated. We found that 1,4 H-shift was thermodynamically more favorable than 1,3-H shift and 1,2-H shift, as was understood through the activation energy barriers for these shifts. The activation energy barriers for the formation of the transition state for 1,4 H-shift was around 14-20 kcal/mol while that for 1,3 H-shift was around 35-40 kcal/mol and 1,2 H-shift was relatively very large (about 61-63 kcal/mol). For unimolecular decomposition channels, the activation energy needed was very high, with a vast range of 65-130 kcal/mol.

Following these computational data, matrix isolation experiments were executed using 2-iodobenzylalcohol as a precursor molecule to form benzyloxyl radical. Unfortunately, we could not see the formation of benzyloxyl radical in matrix isolation conditions, as there was no evidence of radical formation after irradiation with different wavelengths of light. But interestingly, we did observe conformational changes when 2-iodobenzylalcohol was irradiated at 365nm. There were four different conformations possible for 2-iodobenzylalcohol, out of which two of them were

degenerate. The results were similar to the ones on 2-chlorobenzaldehyde which were reported by Nakata et al<sup>20</sup>. In their report on 2-chlorobenzaldehyde, they found similar results like us. The more stable radical isomers were converting into less stable ones upon irradiation of light. Irradiation of the sample at 254 nm after irradiation at 365 nm showed the photoconversion of signals back to its original state. The plausible reason can be either the conformational changes at the excited state, where the barriers can be relatively less or the excitation of the 2-iodobenzyl alcohol upon relaxing undergo hot ground state reaction. Further investigations are needed to understand the reason.

## Chapter 4. Materials and Methods

### 4.1 Computational Details:

We have done the geometry optimization for all possible radical isomers of benzylalcohol (**1a**, **1b**, **1c**, **1d**, and **1e**) and benzylmercaptan (**2a**, **2b**, **2c**, **2d**, and **2e**) including the parent molecule benzylalcohol (**1**) and benzylmercaptan (**2**) at different level of theories. We have used different DFT functionals such as B3LYP, MO6-2X with the cc-pVTZ basis set, and also the composite methods like CBS-QB3 to obtain more accurate thermochemistry data. Apart from that, single-point energy calculations have been performed at (U)CCSD(T) level using already optimized geometries at (U)B3LYP/cc-pVTZ level of theory. We have used unrestricted formalism for all the open-shell species throughout this study. All the minimum energy geometries have been verified with the frequencies calculations, and these calculations were performed using the Gaussian09 suite of programs. The transition states were validated using the imaginary vibrational frequencies in the harmonic approximation calculations.

#### 4.1.1 Methods in Computational Chemistry

Computational chemistry uses computer simulations to help in solving chemical problems using methods of theoretical chemistry. For our work, all calculations are done using the Gaussian09 software package, and for visualization of molecules, gauss view is used. John Pople first released this software in 1970. This software uses different theories like ab-initio, semi-empirical methods, Density Functional Theory (DFT), Quantum Chemistry Composite methods, Coupled Cluster calculations, etc. for doing calculations on molecules such as energy, wavefunctions, orbitals, etc. For our purpose, we will limit ourselves to three of these theories listed below: -

(a) Ab-initio methods: - The term "ab-initio" means "deriving from first principles" which is the basis for this theory as it only inputs physical constants to solve the molecular Schrodinger equation applied with molecular Hamiltonian<sup>21</sup>. This method uses Born-Oppenheimer approximation to find the solution of the electronic Schrodinger equation. Hartree-Fock (HF) method is one of the easiest types of ab-initio process utilized. In this method, correlated electron-

electron repulsion is not explicitly taken into account, but rather an average effect of all other electrons to that particular electron is applied.

(b) Semi-empirical methods: - This method is a combination of the Hartree-Fock process and parameters taken from empirical observation with many other approximations<sup>22</sup>. This method was considered one of the best for calculations concerning large molecules as HF without including the approximations were computationally very costly. The usage of empirical parameters has an added advantage of the inclusion of some correlation terms over the HF method.

(c) Density functional theory (DFT): - This theory uses electron densities to derive molecular properties, unlike semi-empirical and ab-initio methods<sup>23</sup>. DFT is considered to be one of the most efficient and versatile methods for determining the electronic structure of many-body systems. The significant difference in DFT and HF theory is the energy expression terms, while DFT uses electron density to express energy HF uses a linear combination of wavefunctions. There are some methods in which density exchange functional is combined with the HF exchange term to give hybrid functional methods.

We have mainly employed DFT calculations for our systems. Notably, we have exercised the use of B3LYP<sup>24</sup>, which adds a group of approximations from exact exchange from HF theory and other parts from empirical data into the exchange energy correlation functionals. Furthermore, we have used Minnesota functional M06-2X<sup>25</sup> developed by Prof. Donald Truhlar of the University of Minnesota. It is a group of highly parameterized approximate exchange-correlation energy functionals in DFT.

#### **4.1.2 Basis Sets**

Methods like Hartree-Fock, DFT, etc. need to solve electronic wave function, which has partial differential equations. To address these partial differential equations algebraically, one needs to convert these equations into analytically solvable equations. A Basis set<sup>26</sup> is a set of functions that are required to do this job. These can be composed of atomic orbitals, which are then solved using the linear combination of atomic orbitals approach in quantum chemistry. These atomic orbitals can be of many types such as Gaussian-type, Slater atomic orbitals, etc. Gaussian09 uses Gaussian-type orbitals to solve the equations as they give close to accurate results with DFT methods.

Slater-type orbitals (STOs) are physically more reliable to be taken as the solution to the Schrodinger equation but are computationally challenging to solve. Gaussian-type orbitals are considered as a solution to save the computational cost and to get an approximate answer as well. There are different types of Gaussian-type orbital basis set known, which are classified below:-

- (a) Minimal Basis Set:- As the name suggests, these are the smallest basis sets. In this basis set, there is only one basis function given corresponding to one atomic orbital. A very well-known type of minimal basis set is STO-nG<sup>27</sup>, where n is the number of Gaussian primitive functions that contribute to a single basis function. Different kinds of STO-nG are:- STO-3G, STO-4G, STO-6G. These basis sets do not give good results but provide an approximate idea of what the wave function would look like. These have the advantage of reducing computational costs and give close to exact results for gas-phase atom.
- (b) Split-Valence Basis Set: - In most cases of molecular bonding, only valence electrons take part in the bonding, so it makes more sense to represent valence orbitals using more than one basis function. There are many basis sets in which multiple basis functions are given to each valence orbital, and are called valence double, triple, quadruple-zeta, etc<sup>28</sup>. A combination of these orbitals taken into account the spatial environment particular to the molecule, which gives an edge to this basis set in comparison to a minimal basis set that does not take into account different molecular environments.

This basis set is also called Pople basis sets as the group of John Pople gave notation. Examples to this type of basis sets are: - 3-21G<sup>29</sup>, 4-21G, 6-31G, 6-311G, etc. In these types of basis sets, some advancements are also made like 3-21G\* where '\*' signifies the inclusion of polarization effect on heavy atoms. These basis sets are made even more effective by considering the diffusion function on heavy atoms and are denoted by '+' such as 3-21G+.

- (c) Correlation-consistent basis sets: - One of the best basis sets known to date is Correlation-consistent basis sets and, Dunning and coworkers developed these. These are widely known basis sets because these converge Post Hartree-Fock methods to the complete basis sets limit with the aid of empirical data. Basis sets are of the form of cc-pVNZ where N can be =D, T, Q, 5... (D=doublets, T=triplets) and are better used for first- and second-row atoms. Here 'cc' stands for correlation consistent, 'pV' stands for polarized valence-only basis set, and TZ

stands for triple zeta<sup>30</sup>. These are better-suited basis sets as they include polarization functions of successively larger shells like d, f, g,h, etc. Some examples of these types of basis sets are:- cc-pVDZ, cc-pVTZ, cc-pVQZ, cc-pV5Z, aug-cc-pVDZ, aug-cc-pVTZ, etc. These augmented versions of basis sets are an extrapolation of the aforementioned basis sets with added diffusion functions. In our work, we have mainly used cc-pVTZ<sup>31</sup> and DGTZVP for molecules containing higher atoms like Iodine.

#### 4.1.3 Geometry Optimization and Frequency Calculation

Geometry optimization, also known as energy optimization, is a process to find a specific arrangement of atoms in space such that the total inter-atomic force on all the atoms present in the system are in essence, zero. To go by the potential energy surface (PES) terms, it is a stationary point on PES. The geometry of a molecule can be expressed by giving a vector ( $r$ ) to all the atom's positions and then introducing energy as a function of  $r$ ,  $E(r)$ . Thinking about the concept of geometry optimization, mathematically makes more sense as it is the minimum energy that can be found on PES. Now, this minimum can be found using the derivative of the energy function with respect to the position of atoms,  $\partial E/\partial r$ , which should be zero and then the second derivative,  $\partial^2 E/\partial r_i \partial r_j$ , which should be positive for all values.

Frequency calculation is done by using the keyword freq, which will estimate force constants and vibrational frequencies. In addition to that, intensities are also calculated corresponding to that particular frequency. These frequencies are computed by determining the second derivative with respect to the nuclear coordinates. The command opt+freq is given, which calculates the frequencies for the optimized geometry. The use of calculating these frequencies includes knowing different stretches in the molecule and finding the transition state. A true minimum will be the geometry for which all frequency values are positive, while for a transition state, there will be one negative (imaginary) frequency.

In our system, we have done geometry optimization and frequency calculations for all possible radical isomers at B3LYP/cc-pVTZ and M06-2X/cc-pVTZ level of theory. Zero-point energies and enthalpies were calculated at the same level of theories to find the order of relative stability using bond dissociation energy, radical stabilization energy.

#### 4.1.4 Thermochemistry

To get better thermodynamical data, we have also done calculations for bond dissociation energy, radical stabilization energy at CBS-QB3<sup>32</sup> method. This method uses several types of calculations and combines them to give more accurate data. Typically, it combines methods with a high level of theory and a small basis sets with other methods that operate on a lower level of theory with a larger basis set. This method is well known for calculating accurate values of thermodynamical quantities like enthalpy of formation, ionization energies, and electron affinities. The main aim of this type of calculation is to get within 1 kcal/mol of the experimental value.

In a CBS-QB3 calculations, subsequent steps are involved:-

- 1) Optimization and frequency calculations are done at B3LYP/CBSB7 level
- 2) Single point calculations are performed at CCSD(T)<sup>33</sup>/6-31+G(d')<sup>29</sup> level
- 3) Single point calculations are again implemented at MP4SDQ/CBSB4 level
- 4) Total energy is extrapolated to the infinite basis set limit using energies of natural orbitals at the MP2/CBSB3 level and a correction to the CCSD(T) level.

## 4.2 Experimental Set-up

### 4.2.1 Matrix Isolation Technique

Matrix isolation is a technique that is used for managing the molecule at cryogenic environments using vacuum conditions for spectroscopic study on the guest molecule. This technique is typically suited for the trapping of reactive intermediates like radicals, carbocations, carbenes, nitrenes, etc. The precursor molecule is trapped inside an unreactive matrix. This unreactive matrix is made up of an inert gas which is chemically unreactive with the molecule of interest. Typically, the concentration ratio of the inert gas to the precursor molecules is taken to be 1000:1 or 2000:1. This method holds an edge over the other methods as it stabilizes the reactive intermediate. Furthermore, the isolation of precursor molecules in the inert matrix reduces the probability of intermolecular interactions. The cryogenic conditions used in this process helps in the inhibition



of any other processes as energy at such low temperature would be very small to pass through the activation energy barriers for most reactions. The mixture of the guest molecule and highly unreactive gas is then made to be in contact with a surface at a very low temperature so that the reactive species can be kinetically trapped inside the cavities of the host matrix. George C. Pimentel developed the technique of matrix isolation and is also known as the "Father of matrix isolation." This technique has been used in conjunction with various spectroscopic techniques: Infrared, UV-Vis, Raman, NMR, etc. So this technique helps us to get insights about the molecular properties in an isolated condition without the presence of intermolecular interactions.

#### **4.2.2 Frequency Shift**

We compare the frequencies of computational spectrums to frequencies of experimentally generated spectrums to confirm the presence of radicals in isolated conditions. But the values of frequency in experimental spectrums are generally shifted from that of computational values as the spectrums generated using computation are for gas-phase conditions. But real-time experiment frequencies get shifted because of the presence of Van der Waals, electrostatic, repulsive interactions. In general, below  $1000\text{ cm}^{-1}$ , the experimental spectra is blue-shifted from computed spectra, and above  $1000\text{ cm}^{-1}$ , it is red-shifted.

#### **4.2.3 Set-up of Matrix Isolation Technique and its Functioning**

The experimental setup contains Rotary vane and diffusion pumps, Spectrophotometer, Flow controller, Helium Compressor, Deposition unit, KBr window. All these different pieces of equipment have been described in the following paragraphs. The experiments were carried at a pressure in realms of  $10^{-6}$  mbar, which was reached with the help of rotary vane and diffusion pump. Before the setup of experiments, the chamber pressure was brought down from room pressure (1.01 bar) to the range of  $10^{-3}$ - $10^{-4}$  mbar using rotary vane pump. Then this pressure was further decreased to  $5.0$ - $6.0 \times 10^{-5}$  mbar using diffusion pump at room temperature (298K). After this temperature of cryostat was made to go from 298K to 4K using Sumitomo helium compressor by keeping setup point as 4K. Chillers are used to take the heat out of both the diffusion pump and closed-cycle helium compressor. Then the background spectrum is recorded using Bruker's FTIR

spectrophotometer using 128 or 256 scans with the purging of nitrogen gas. The spectrum is recorded at a resolution of  $0.5\text{ cm}^{-1}$  traversing from  $400\text{ cm}^{-1}$  to  $4000\text{ cm}^{-1}$ . Mass flow controller (MFC) was used to control the flow of the host gas at 5 sccm (standard cubic centimeter per minute).

#### **4.2.3.1 Rotary Vane and Diffusion Pumps**

We use two different types of pumps - Oil Sealed Rotary Vane and Diffusion pump to maintain the pressure of  $10^{-6}$  mbar, which is necessary for our setup to function correctly. Generally, room temperature is 1.01 bar, which has to be brought down to  $10^{-6}$  mbar. Firstly, the oil sealed rotary vane pump (model number RV12) is used to bring down the pressure until the range of  $10^{-3}$  mbar. This pump operates on 50 Hz ac supply with 1430rpm, and the cold cathode gauge is used to measure the pressure. Then, for the pressure to go down to the range of  $10^{-6}$  mbar, a diffusion pump is used. This pressure is measured by Pirani and Penning gauge (model: Edward APG 100 active). Maintaining high pressure is necessary as it tells us the purity of the experiment. Lesser pressure implies better vacuum condition, which in turn suggests a lower level of impurities inside the cryostat.

#### **4.2.3.2 Spectrophotometer**

A spectrophotometer is a tool that is used to do a quantitative analysis of molecules depending upon how much light a molecule will absorb as a function of wavelength or wavenumber. Two types of spectrophotometer are there: Single beam and double beam spectrophotometer. The main part in a spectrophotometer is Michelson interferometer which has a beam splitter, one fixed and one oscillating mirror. To record the FTIR spectrum in our experiments, we have used Bruker's spectrophotometer (model: Tensor II), which has a resolution limit of  $0.49\text{ cm}^{-1}$ . But for our experiments, we have recorded the spectrum at a resolution of  $0.5\text{ cm}^{-1}$ . In most of our experiments, we used 128 or 256 scans, which has some advantages. One of them is that high scanning rates allow us for rapid sample processing with an added advantage of reducing the random errors in the collected spectra (better signal to noise ratio).

#### **4.2.3.3 Flow Controller**

Matrix gas is one of the essential parts of the setup, so to choose the type of matrix gas becomes necessary. We can select any gas as the host gas as long as it is spectroscopically transparent in the region of our interest. Furthermore, this gas should be inert or have almost no interaction with the precursor molecule. Gases with these properties would be ideal for our concern. There are some gases like Neon, Argon, and Nitrogen, which could potentially be used as a matrix gas.

We have used Nitrogen and Argon as host gases in our experiments. These are of 99.999% purity, and their flow can be measured and controlled by Mass Flow Controller (mks-MFC GE50A). The matrix gases can flow through this flow controller and makeup the inert matrix. The flow can be varied from 5sccm to 10sccm.

#### **4.2.3.4 Helium Compressor**

The experiments were conducted at 4K, but for annealing, we went up to 30K. To maintain this temperature at the head and KBr window, a closed cycle helium compressor is used, which works on the principle of Joule Thompson effect. For this cooling purpose, H<sub>2</sub>, He or Ne can be used because these gases cool down on expansion at room temperature as their Z (compressibility factor) is less than one. We use the compressor which uses helium as the gas with a three-step cycle. For this cycle, gas was pumped at 190-200 psi through the inlet and was expanded in the head. Then it was made to leave through the outlet pipe back to the compressor where it was compressed again. The heat from the compressor was extracted out by chiller operating at 12 kW power.

#### **4.2.3.5 Deposition Unit and KBr Window**

The deposition unit is thermally conducting and is insulated for vacuum by using O-ring and connecting units, in which our analyte molecule is placed. The KBr window has a diameter of 25 mm and a thickness of 4 mm on which the precursor molecule, along with host gas, is deposited.

This window is at a temperature of 4K and is held by copper linking to the cryotip. The window at which the molecule is deposited is also vacuum isolated, which is done using the O-rings and rotatable metallic jacket.

This metallic jacket has four sides, out of which two sides have KBr windows (that are transparent for IR radiation), one side has a quartz window (which is transparent to UV-Vis radiation), and the fourth side is directly connected to the deposition unit. The quartz window, which is transparent to UV-Vis radiation, is used to irradiate the molecule for discovering the photochemistry of molecules.

#### 4.2.4 Matrix Isolation FT-IR Facility in POC Lab at IISER Mohali

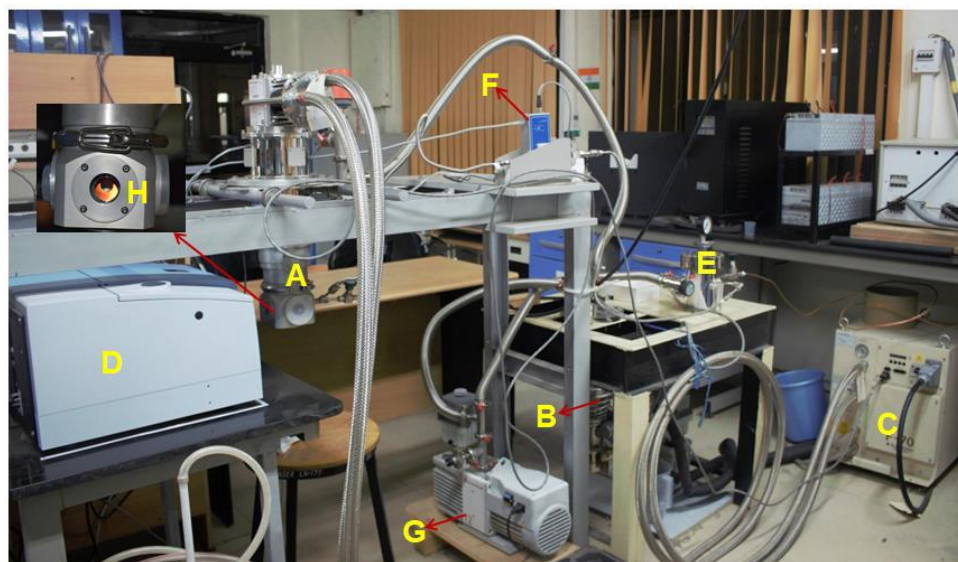


**Figure 4.1:** Matrix isolation set up.

- |                            |                          |                             |
|----------------------------|--------------------------|-----------------------------|
| <b>A:</b> Cryostat         | <b>B:</b> Diffusion pump | <b>C:</b> Helium compressor |
| <b>D:</b> IR spectrometer  | <b>E:</b> Mixing chamber | <b>F:</b> Flow controller   |
| <b>G:</b> Rotary vane pump | <b>H:</b> KBr window     |                             |

# References

1. Hayyan, M.; Hashim, M.A.; AlNashef, I.M. Superoxide Ion: Generation and Chemical Implications. *Chem. Rev.* **2016**, *116* (5), 3029-85.
2. Gomberg, M. Organic Radicals. *Chem. Rev.* **1924**, *1* (1), 91–141.
3. Cochran, E. L.; Adrian, F. J.; Bowers, V. A. ESR Study of Ethynyl and Vinyl Free Radicals. *J. Chem. Phys.* **1964**, *40*, 213.
4. Romero, N. A.; Nicewicz, D. A. Organic Photoredox Catalysis. *Chem. Rev.*, **2016**, *116* (17), 10075–10166.
5. Lave, T.; Plagens A.; Named Organic Reactions, Second Edition. *J. Chem. Edu.*, **2005**, *82*(12), 1780-1781.
6. Matyjaszewski, K.; Xia, J. Atom Transfer Radical Polymerization. *Chem. Rev.*, **2001**, *101* (9), 2921–2990.
7. Khelifa, F.; Ershov, S.; Habibi, Y.; Snyders, R.; Dubois, P. Free-Radical-Induced Grafting from Plasma Polymer Surfaces. *Chem. Rev.*, **2016**, *116* (6), 3975–4005.
8. Orlando, J. J.; Tyndall, G. S.; Wallington, T. J. The Atmospheric Chemistry of Alkoxy Radicals. *Chem. Rev.* **2003**, *103* (12), 4657–4690.
9. Gligorovski, S.; Strekowski, R.; Barbati, S.; Vione, D. Environmental Implications of Hydroxyl Radicals ( $\bullet\text{OH}$ ). *Chem. Rev.*, **2015**, *115* (24), 13051–13092.
10. Duarte, L.; Rekola, I.; Khriachtchev, L. Complex between Formic Acid and Nitrous Oxide: A Matrix-Isolation and Computational Study. *J. Phys. Chem. A*, **2017**, *121* (45), 8728–8737.
11. Pacher P.; Beckman J. S.; Liaudet L. Nitric oxide and peroxynitrite in health and disease. *Physiol. Rev.*, **2007**, *87* (1), 315–424.
12. Floyd, R.A. Neuroinflammatory processes are important in neurodegenerative diseases: A hypothesis to explain the increased formation of reactive oxygen and nitrogen species as major factors involved in neurodegenerative disease development. *Free Radic. Biol. Med.*, **1999**, *26* (9–10), 1346–55.
13. Karthikeyan, R.; Manivasagam T.; Anantharaman P.; Balasubramanian T.; Somasundaram S. T. Chemopreventive effect of *Padina boergesii* extracts on ferric nitrilotriacetate (Fe-NTA)-induced oxidative damage in Wistar rats. *J. Appl. Phycol.*, **2011**, *23* (2), 257–63.

14. Mukherjee, P. K.; Marcheselli, V. L.; Serhan, C. N.; Bazan, N. G. Neuroprotectin D1: A docosahexanoic acid-derived docosatriene protects human retinal pigment epithelial cells from oxidative stress. *Proc. Natl. Acad. Sci. U.S.A.*, **2004**, *101*(22), 8491–96.
15. Silva, G. D.; Hamdan, M. R.; Bozzelli, J. W. Oxidation of the Benzyl Radical: Mechanism, Thermochemistry, and Kinetics for the Reactions of Benzyl Hydroperoxide. *J. Chem. Theory Comput.*, **2009**, *5* (12), 3185–3194.
16. Silva, G. D.; Cole, J. A.; Bozzelli, J. W. Thermal Decomposition of the Benzyl Radical to Fulvenallene (C<sub>7</sub>H<sub>6</sub>) H. *J. Phys. Chem. A*, **2009**, *113* (21), 6111–6120.
17. Dyakov, Y. A. Photodissociation dynamics of benzyl alcohol at 193 nm. *J. Chem. Phys.*, **2012**, *137* (6), 064314.
18. Hoomissen, D. J. V.; Vyas, S. 1,2-H Atom Rearrangements in Benzyloxy Radicals. *J. Phys. Chem. A*, **2018**, *123* (2), 492–504.
19. Simons, J. P.; Robertson, E. G.; Mons, M. Intra- and Intermolecular  $\pi$ -Type Hydrogen Bonding in Aryl Alcohols: UV and IR-UV Ion Dip Spectroscopy. *J. Phys. Chem. A*, **2000**, *104*, 1430-1437.
20. Akai, N., Kudoh, S., Takayanagi, M., & Nakata, M. Photoinduced rotational isomerization mechanism of 2-chlorobenzaldehyde in low-temperature rare-gas matrices by vibrational and electronic spectroscopies. *J. Photochem. Photobiol.*, **2002**, *150* (1-3), 93–100.
21. Parr, R. G.; Craig, D. P.; Ross, I. G. Molecular Orbital Calculations of the Lower Excited Electronic Levels of Benzene, Configuration Interaction Included. *J. Chem. Phys.* **1950**, *18* (12), 1561–1563.
22. Hoffmann, R. An Extended Hückel Theory. I. Hydrocarbons. *J. Chem. Phys.* **1963**, *39* (6), 1397–1412.
23. Grimme, S. Semiempirical Hybrid Density Functional with Perturbative Second-Order Correlation. *J. Chem. Phys.* **2006**, *124* (3), 034108.
24. Becke, A. D. Density-functional Thermochemistry. III. The Role of Exact Exchange. *J. Chem. Phys.* **1993**, *98* (7), 5648–5652.
25. Zhao, Y.; Truhlar, D. G. The M06 Suite of Density Functionals for Main Group Thermochemistry, Thermochemical Kinetics, Noncovalent Interactions, Excited States, and Transition Elements: Two New Functionals and Systematic Testing of Four M06-Class Functionals and 12 Other Functionals. *Theor. Chem. Acc.* **2008**, *120* (1–3), 215–241.

26. House, J. E.; House, J. E. Comments on Computational Methods. *Fundam. Quantum Mech.* **2018**, 335–347.
27. Watson, T. J.; Chan, G. K.-L. Correct Quantum Chemistry in a Minimal Basis from Effective Hamiltonians. *J. Chem. Theory Comput.* **2016**, 12 (2), 512–522.
28. Wallace, A. J.; Crittenden, D. L. Optimal Composition of Atomic Orbital Basis Sets for Recovering Static Correlation Energies. **2014**.
29. McLean, A. D.; Chandler, G. S. Contracted Gaussian Basis Sets for Molecular Calculations. I. Second Row Atoms,  $Z = 11-18$ . *J. Chem. Phys.* **1980**, 72 (10), 5639–5648.
30. Hofer, T. S. On the Basis Set Convergence of Electron–electron Entanglement Measures: Helium-like Systems. *Front. Chem.* **2013**, 1, 24.
31. Krishnan, R.; Binkley, J. S.; Seeger, R.; Pople, J. A. Self-consistent Molecular Orbital Methods. XX. A Basis Set for Correlated Wave Functions. *J. Chem. Phys.* **1980**, 72 (1), 650–654.
32. Range, K.; Riccardi, D.; Cui, Q.; Elstner, M.; York, D. M. Benchmark Calculations of Proton Affinities and Gas-Phase Basicities of Molecules Important in the Study of Biological Phosphoryl Transfer. *Phys. Chem. Chem. Phys.* **2005**, 7 (16), 3070.
33. Ghigo, G.; Tonachini, G. Density Functional, Single and Multireference Perturbation Theory Study of the Reaction  $3\Sigma_gO_2+HOCH_2CH_2\cdot\rightarrow HOO\cdot+HOCH=CH_2$ , Modeling an Important Step in Tropospheric Benzene Oxidation. *J. Chem. Phys.* **1999**, 110 (15), 7298–7304.

## Appendix

**Table A1:** Electronic and thermodynamic parameters of all the complexes at (U)B3LYP/cc-pVTZ (bold) and (U)M06-2X/cc-pVTZ (normal font).

Species	Absolute Energy (Hartree)	ZPVE (Hartree)	Lowest frequency	Spin Contamination		Point group	Electronic state	Free Energy (Hartree)	Enthalpy (Hartree)
				Before annihilation	After annihilation				
<b>1</b>	<b>-346.772189</b>	<b>0.133129</b>	<b>44.4</b>	<b>0.0000</b>	<b>0.0000</b>	<b>C<sub>1</sub></b>	<b><sup>1</sup>A</b>	<b>-346.804015</b>	<b>-346.764217</b>
	-346.618709	0.134706	55.3	0.0000	0.0000	C <sub>1</sub>	<sup>1</sup> A	-346.650277	-346.610830
<b>1a</b>	<b>-346.096334</b>	<b>0.120015</b>	<b>49.0</b>	<b>0.7568</b>	<b>0.7500</b>	<b>C<sub>1</sub></b>	<b><sup>2</sup>A</b>	<b>-346.128662</b>	<b>-346.088397</b>
	-345.946064	0.121592	57.3	0.7616	0.7500	C <sub>1</sub>	<sup>2</sup> A	-345.978186	-345.938225
<b>1b</b>	<b>-346.096334</b>	<b>0.120015</b>	<b>49.0</b>	<b>0.7568</b>	<b>0.7500</b>	<b>C<sub>1</sub></b>	<b><sup>2</sup>A</b>	<b>-346.128662</b>	<b>-346.088397</b>
	-345.946064	0.121592	57.3	0.7620	0.7500	C <sub>1</sub>	<sup>2</sup> A	-345.978186	-345.938225
<b>1c</b>	<b>-346.095524</b>	<b>0.120036</b>	<b>42.8</b>	<b>0.7570</b>	<b>0.7500</b>	<b>C<sub>1</sub></b>	<b><sup>2</sup>A</b>	<b>-346.087575</b>	<b>-346.087575</b>
	-345.945330	0.121619	55.6	0.7620	0.7500	C <sub>1</sub>	<sup>2</sup> A	-345.977490	-345.937476
<b>1d</b>	<b>-346.146164</b>	<b>0.119484</b>	<b>95.6</b>	<b>0.7754</b>	<b>0.7504</b>	<b>C<sub>1</sub></b>	<b><sup>2</sup>A</b>	<b>-346.177919</b>	<b>-346.138250</b>
	-345.991143	0.120762	83.4	0.7749	0.7504	C <sub>1</sub>	<sup>2</sup> A	-346.022972	-345.983248
<b>1e</b>	<b>-346.114994</b>	<b>0.117968</b>	<b>35.6</b>	<b>0.7542</b>	<b>0.7500</b>	<b>C<sub>s</sub></b>	<b><sup>2</sup>A''</b>	<b>-346.147515</b>	<b>-346.107158</b>
	-345.958531	0.119546	27.8	0.7543	0.7500	C <sub>s</sub>	<sup>2</sup> A''	-345.991195	-345.950776
<b>2</b>	<b>-669.755753</b>	<b>0.127714</b>	<b>37.4</b>	<b>0.0000</b>	<b>0.0000</b>	<b>C<sub>s</sub></b>	<b><sup>1</sup>A'</b>	<b>-669.788957</b>	<b>-669.747234</b>
	-669.594142	0.128789	15.4	0.0000	0.0000	C <sub>s</sub>	<sup>1</sup> A	-669.628440	-669.585495
<b>2a</b>	<b>-669.079426</b>	<b>0.114671</b>	<b>15.0</b>	<b>0.7569</b>	<b>0.7500</b>	<b>C<sub>1</sub></b>	<b><sup>2</sup>A</b>	<b>-669.113383</b>	<b>-669.070884</b>
	-668.920272	0.116178	25.9	0.7618	0.7500	C <sub>1</sub>	<sup>2</sup> A	-668.954229	-668.911897
<b>2b</b>	<b>-669.079494</b>	<b>0.114572</b>	<b>36.2</b>	<b>0.7569</b>	<b>0.7500</b>	<b>C<sub>1</sub></b>	<b><sup>2</sup>A</b>	<b>-669.113350</b>	<b>-669.070981</b>
	-668.920925	0.115859	24.0	0.7620	0.7500	C <sub>1</sub>	<sup>2</sup> A	-668.955166	-668.912427
<b>2c</b>	<b>-669.079026</b>	<b>0.114602</b>	<b>37.6</b>	<b>0.7571</b>	<b>0.7500</b>	<b>C<sub>1</sub></b>	<b><sup>2</sup>A</b>	<b>-669.112806</b>	<b>-669.070532</b>
	-668.921022	0.115428	14.8	0.7622	0.7501	C <sub>1</sub>	<sup>2</sup> A	-668.955103	-668.913120
<b>2d</b>	<b>-669.128030</b>	<b>0.114402</b>	<b>81.2</b>	<b>0.7732</b>	<b>0.7504</b>	<b>C<sub>s</sub></b>	<b><sup>2</sup>A''</b>	<b>-669.161066</b>	<b>-669.119584</b>
	-668.964693	0.115769	94.1	0.7713	0.7503	C <sub>s</sub>	<sup>2</sup> A''	-668.997388	-668.956422
<b>2e</b>	<b>-669.121020</b>	<b>0.117527</b>	<b>42.2</b>	<b>0.7539</b>	<b>0.7500</b>	<b>C<sub>s</sub></b>	<b><sup>2</sup>A''</b>	<b>-669.152567</b>	<b>-669.113866</b>
	-668.961962	0.118431	44.6	0.7537	0.7500	C <sub>s</sub>	<sup>2</sup> A''	-668.993526	-668.954756



**Table A2:** Experimental and computational infrared data of 2-iodobenzylalcohol

S. No.	Experimental (Ar, 4 K)		Conformation - 1 & 2		Conformation - 3		Conformation - 4		Normal mode / (Symmetry)
	Wavenumber (cm <sup>-1</sup> )	Rel. Intensity	Wavenumber (cm <sup>-1</sup> )	Rel. Intensity	Wavenumber (cm <sup>-1</sup> )	Rel. Intensity	Wavenumber (cm <sup>-1</sup> )	Rel. Intensity	
1	–	–	75.6	4.0	79.6	3.0	78.6	3.1	A
2	–	–	111.4	0.8	125.3	0.6	125.0	0.7	A
3	–	–	158.4	1.3	146.2	0.1	146.2	0.1	A
4	–	–	200.8	1.7	210.8	3.0	210.5	3.0	A
5	–	–	243.3	1.0	240.0	0.9	240.0	0.9	A
6	–	–	329.0	35.7	284.1	2.5	284.1	2.5	A
7	–	–	359.4	100.0	346.7	100.0	344.7	100.0	A
8	–	–	409.9	44.5	435.4	3.4	435.4	3.4	A
9	–	–	449.3	7.1	449.8	2.1	449.8	2.0	A
10	–	–	510.4	2.3	502.4	1.3	502.3	1.3	A
11	600, 603	12, 7	606.6	19.2	600.9	2.8	600.9	2.8	A
12	650, 657	13, 21	653.5	19.3	660.9	8.4	660.9	8.5	A
13	721	9	730.1	10.1	707.7	1.7	707.6	1.7	A
14	747,749,751	45, 71, 100	758.4	83.9	758.5	42.5	758.3	42.5	A
15	760	12	825.8	6.4	801.7	2.3	801.7	2.3	A
16	938	14	876.3	1.1	877.0	0.7	876.8	0.7	A
17	950	51	952.0	4.3	952.3	5.5	952.2	5.5	A
18	973	10	964.4	36.1	986.0	11.8	985.9	11.9	A
19	982	10	989.8	0.1	996.5	3.5	996.4	3.4	A
20	1015, 1017	82, 63	1016.0	62.9	1017.4	46.6	1017.4	46.7	A
21	1028	57	1050.2	100.0	1065.4	10.9	1065.5	10.9	A
22	1031	47	1070.1	24.8	1076.5	41.9	1076.5	41.9	A
23	1044, 1048, 1051	19, 24, 29	1133.3	19.6	1138.1	9.2	1138.1	9.2	A
24	1060, 1062	56, 30	1182.8	0.3	1180.8	0.1	1180.7	0.1	A
25	1115	15	1200.9	63.6	1215.5	1.5	1215.4	1.8	A
26	1175,1178	30, 32	1221.6	28.7	1218.8	19.8	1218.8	19.6	A
27	1209	33	1304.0	5.1	1285.2	2.2	1285.1	2.2	A

28	1294	33	1336.4	20.8	1321.3	2.1	1321.4	2.1	A
29	1342	22	1377.7	11.0	1390.1	4.2	1389.9	4.1	A
30	1383	34	1425.3	82.8	1411.8	39.4	1411.7	39.3	A
31	1441	38	1463.2	23.9	1462.2	15.5	1462.2	15.5	A
32	1455	24	1492.4	19.8	1486.5	14.8	1486.6	14.7	A
33	1570	29	1512.7	9.7	1502.8	1.1	1502.8	1.2	A
34	1592	30	1612.6	17.1	1612.1	9.0	1612.1	9.1	A
35	–	–	1635.0	10.1	1635.9	2.9	1636.0	2.9	A
36	2874, 2885	4, 6	3043.6	49.2	3041.6	15.3	3042.6	15.2	A
37	2918	3	3133.0	34.1	3107.9	7.0	3108.3	7.0	A
38	2983, 2989	3, 4	3184.4	4.4	3189.2	1.5	3189.5	1.5	A
39	3019	2	3195.8	11.9	3203.1	5.4	3203.4	5.5	A
40	3063, 3073, 3082	4, 7, 3	3209.9	19.3	3213.8	4.4	3214.2	4.3	A
41	–	–	3220.9	11.0	3220.2	6.3	3220.4	6.4	A
42	3595,3600,3605, 3607	20, 17, 13, 12	3739.6	42.4	3766.5	19.5	3767.9	19.5	A

**Table A3:** Cartesian Co-ordinates of Selected Species

(U)B3LYP/cc-pVTZ				(U)M06-2X/cc-pVTZ			
<b>1</b>				<b>1</b>			
C	0.000040302	-0.000013342	0.000010484	C	0.000013530	-0.000001945	0.000002281
C	-0.000014900	-0.000016899	-0.000005235	C	-0.000005277	-0.000014645	0.000004913
C	-0.000000399	0.000016992	0.000001858	C	0.000003618	0.000015432	-0.000003353
C	0.000008704	-0.000010822	-0.000001565	C	0.000009041	0.000008179	0.000009300
C	0.000013625	-0.000020699	0.000004205	C	-0.000011348	0.000005917	-0.000006263
C	-0.000079107	0.000055050	-0.000014794	C	0.000013195	-0.000011796	-0.000007019
H	-0.000004574	-0.000002586	-0.000002409	H	-0.000001545	-0.000002119	-0.000001141
H	0.000003883	-0.000002600	0.000000101	H	0.000003244	0.000003326	-0.000000716
H	0.000003325	0.000002490	0.000001145	H	0.000000543	0.000004053	-0.000001839
H	-0.000000233	0.000006120	0.000000812	H	-0.000002178	0.000003859	-0.000002761
H	-0.000002038	0.000007323	-0.000000614	H	-0.000004398	-0.000000945	0.000004204
C	0.000048841	-0.000021795	0.000033596	C	-0.000049161	0.000042661	0.000007630
H	-0.000008215	-0.000005033	-0.000005453	H	0.000001297	-0.000012488	-0.000001768
H	-0.000007147	0.000006791	-0.000014047	H	0.000007215	-0.000019038	-0.000002683
O	0.000005066	0.000005564	0.000020194	O	0.000039871	-0.000016195	-0.000003383
H	-0.000007134	-0.000006553	-0.000028277	H	-0.000017647	-0.000004255	0.000002599
<b>1a</b>				<b>1a</b>			
C	-0.000013738	0.000020698	0.000001648	C	0.000001843	-0.000000504	-0.000001015
C	0.000016589	0.000000862	0.000002368	C	0.000001850	-0.000002950	-0.000001211
C	-0.000008641	-0.000013772	-0.000001264	C	-0.000000352	-0.000003235	0.000000275
C	-0.000007365	0.000008896	0.000007498	C	-0.000002916	-0.000003290	0.000001911
C	0.000004661	0.000010144	-0.000003555	C	-0.000001450	-0.000000478	0.000001308
C	0.000001997	-0.000036164	0.000000232	C	0.000000226	0.000002182	-0.000000375
H	0.000000849	-0.000002956	-0.000001090	H	0.000003533	0.000000645	-0.000002500
H	-0.000000379	-0.000000114	-0.000001467	H	0.000002981	-0.000003765	-0.000002004
H	0.000002257	0.000002093	-0.000001238	H	-0.000000799	-0.000005760	0.000000557
H	0.000000703	0.000001205	-0.000002095	H	-0.000004044	-0.000003340	0.000002789
C	0.000005994	0.000023475	-0.000002401	C	0.000000049	0.000004134	-0.000000072
H	-0.000001069	-0.000006302	0.000003886	H	0.000000902	0.000005188	-0.000000711
H	0.000000859	-0.000004070	0.000000594	H	0.000001972	0.000003497	-0.000001458
O	-0.000003156	-0.000004589	0.000006720	O	-0.000001933	0.000004409	0.000001248
H	0.000000440	0.000000594	-0.000009837	H	-0.000001862	0.000003268	0.000001256
<b>1b</b>				<b>1b</b>			
C	0.000016542	0.000006580	-0.000006827	C	-0.000004531	-0.000003733	-0.000000541
C	-0.000008897	0.000007320	0.000010672	C	0.000005180	-0.000006825	0.000001396
C	-0.000008696	-0.000011821	-0.000006342	C	0.000001665	-0.000001789	0.000000776
C	0.000011846	-0.000000268	-0.000000775	C	-0.000010337	-0.000000729	0.000003123
C	-0.000003865	0.000013245	0.000006128	C	0.000004039	-0.000007554	-0.000000016
C	-0.000021962	-0.000019082	0.000000512	C	0.000000577	0.000007905	0.000000507
H	-0.000001696	-0.000000958	0.000000097	H	0.000005198	-0.000000231	-0.000001812
H	0.000001062	-0.000002449	-0.000000183	H	0.000002620	-0.000004897	0.000000804
H	0.000000929	0.000001344	0.000001355	H	-0.000002141	-0.000007338	0.000003423
C	0.000049889	0.000041440	0.000015390	C	0.000000443	0.000003195	-0.000003211
H	-0.000002442	-0.000003210	-0.000004155	H	0.000000148	0.000004983	-0.000001936
H	-0.000003851	-0.000004451	0.000000136	H	0.000003062	0.000004711	-0.000002471
O	-0.000031942	-0.000028069	-0.000013263	O	-0.000000833	0.000005748	-0.000000087
H	0.000004428	0.000000321	-0.000000396	H	-0.000000247	0.000004185	-0.000001290
H	-0.000001347	0.000000059	-0.000002349	H	-0.000004841	0.000002368	0.000001336
<b>1c</b>				<b>1c</b>			
C	0.000000036	-0.000000994	0.000000766	C	0.000032888	0.000010795	0.000005433
C	-0.000000033	-0.000000431	-0.000000577	C	-0.000031284	0.000023874	0.000004209

C	-0.000000087	-0.000000682	-0.000000068	C	-0.000002466	-0.000026146	-0.000000083
C	0.000001343	-0.000000206	0.000000225	C	0.000032833	0.000015171	0.000000733
C	-0.000001518	0.000001376	-0.000000008	C	-0.000018614	0.000018390	0.000005190
C	0.000001099	0.000000204	-0.000000488	C	-0.000014188	-0.000029785	-0.000011005
H	0.000000939	0.000000273	0.000000002	H	-0.000006832	0.000000166	-0.000000704
H	0.000000192	-0.000000206	-0.000000016	H	-0.000002467	0.000004700	0.000000191
H	-0.000001002	-0.000000585	-0.000000194	H	-0.000000288	0.000000924	-0.000000059
H	0.000000237	-0.000000469	-0.000000074	H	0.000006582	-0.000003551	-0.000000641
C	-0.000003295	-0.000001564	-0.000001432	C	0.000019188	0.000023186	-0.000004502
H	0.000000255	0.000000051	-0.000000081	H	-0.000001824	-0.000010482	0.000005406
H	0.000000482	0.000000311	0.000000029	H	-0.000004433	-0.000006183	-0.000000298
O	0.000001439	0.000002218	0.000001466	O	-0.000013775	-0.000018629	0.000000776
H	-0.000000087	0.000000705	0.000000449	H	0.000004682	-0.000002431	-0.000004648
<b>1d</b>				<b>1d</b>			
C	-0.000002149	0.000002230	0.000000163	C	0.000110079	0.000054053	0.000000013
C	0.000000259	0.000002393	-0.000000628	C	-0.000110584	0.000162906	0.000000016
C	-0.000006054	-0.000006804	0.000000139	C	-0.000032023	-0.000117739	-0.000000041
C	0.000009608	0.000002037	0.000000367	C	-0.000267618	-0.000078001	-0.000000034
C	-0.000005865	0.000002444	-0.000001350	C	0.000418836	0.000168561	-0.000000019
C	0.000003930	-0.000007229	0.000001212	C	-0.000454323	-0.000126050	0.000000201
H	0.000001039	-0.000000513	0.000000256	H	0.000000613	0.000012195	-0.000000020
H	0.000000674	-0.000001293	0.000000350	H	-0.000005931	0.000010018	-0.000000010
H	0.000000418	-0.000000420	-0.000000109	H	-0.000030962	-0.000001307	0.000000044
H	-0.000000979	-0.000000355	-0.000000290	H	0.000007432	-0.000023710	-0.000000019
H	0.000000214	0.000001962	0.000000819	H	0.000012604	-0.000045348	0.000000106
C	0.000000396	0.000004321	-0.000001650	C	0.000668464	-0.000135236	-0.000000192
H	-0.000000542	-0.000000511	0.000000598	H	-0.000109752	0.000057924	-0.000000149
O	-0.000000354	0.000001096	-0.000001097	O	-0.000191060	0.000164985	0.000000669
H	-0.000000594	0.000000643	0.000001220	H	-0.000015777	-0.000103250	-0.000000566
<b>1e</b>				<b>1e</b>			
C	0.000007214	0.000005113	0.000000000	C	0.000005758	-0.000002144	0.000000000
C	-0.000003180	0.000004389	0.000000000	C	0.000003799	-0.000005257	0.000000000
C	0.000001069	-0.000007569	0.000000000	C	-0.000002204	-0.000010013	0.000000000
C	0.000000432	0.000001683	0.000000000	C	-0.000002775	-0.000003779	0.000000000
C	-0.000002028	0.000006406	0.000000000	C	-0.000006300	0.000001463	0.000000000
C	-0.000000305	-0.000011348	0.000000000	C	-0.000002173	0.000003224	0.000000000
H	-0.000000434	-0.000000927	0.000000000	H	0.000008250	0.000001209	0.000000000
H	0.000001639	-0.000002179	0.000000000	H	0.000006787	-0.000008869	0.000000000
H	-0.000001467	-0.000002334	0.000000000	H	-0.000001965	-0.000012205	0.000000000
H	-0.000001064	-0.000001633	0.000000000	H	-0.000010484	-0.000006305	0.000000000
H	-0.000001989	-0.000000230	0.000000000	H	-0.000007929	0.000003297	0.000000000
C	-0.000010116	-0.000001074	0.000000000	C	0.000002394	0.000008265	0.000000000
H	0.000002189	0.000001691	-0.000002428	H	0.000004330	0.000009766	-0.000000908
H	0.000002189	0.000001691	0.000002428	H	0.000004330	0.000009766	0.000000908
O	0.000005852	0.000006320	0.000000000	O	-0.000001819	0.000011582	0.000000000
<b>2</b>				<b>2</b>			
C	0.000022059	-0.000013164	0.000000000	C	-0.000001791	0.000000200	0.000003880
C	-0.000016789	0.000016852	-0.000000157	C	0.000001250	-0.000002224	0.000002947
C	0.000001082	-0.000051667	-0.000013635	C	0.000001589	-0.000001731	0.000000520
C	0.000059123	0.000069197	0.000000000	C	0.000000432	0.000000600	-0.000001143
C	0.000001082	-0.000051667	0.000013635	C	-0.000002235	0.000002769	-0.000000329
C	-0.000016789	0.000016852	0.000000157	C	-0.000003203	0.000001666	0.000002382
H	0.000000388	0.000001566	0.000000000	H	-0.000002589	0.000000364	0.000005634
H	-0.000000509	0.000002012	-0.000001058	H	0.000001822	-0.000003270	0.000003422
H	0.000002841	0.000002334	0.000002037	H	0.000003931	-0.000003721	-0.000000823

H	0.000002841	0.000002334	-0.000002037	H	-0.000003428	0.000003552	-0.000000633
H	-0.000000509	0.000002012	0.000001058	H	-0.000005332	0.000004085	0.000003584
C	-0.000069504	-0.000042617	0.000000000	C	0.000002960	0.000000117	-0.000002287
H	0.000010662	-0.000002609	0.000002986	H	0.000003412	-0.000001068	-0.000004827
H	0.000010662	-0.000002609	-0.000002986	H	0.000000324	0.000001962	-0.000005589
S	0.000004460	0.000044420	0.000000000	S	0.000000631	-0.000001073	-0.000005705
H	-0.000011100	0.000006754	0.000000000	H	0.000002227	-0.000002229	-0.000001033
<b>2a</b>				<b>2a</b>			
C	0.000020890	-0.000010582	-0.000016617	C	0.000001724	-0.000001229	0.000000368
C	-0.000037706	0.000033903	-0.000013539	C	0.000002404	-0.000002404	0.000000411
C	0.000062159	-0.000046490	0.000027612	C	0.000000762	-0.000003723	0.000004110
C	-0.000078095	0.000037052	-0.000095345	C	-0.000000739	0.000006295	-0.000000608
C	0.000061995	0.000006543	0.000011407	C	0.000002159	-0.000002782	-0.000001961
C	-0.000023140	0.000000074	0.000020166	C	-0.000004261	-0.000004127	-0.000002306
H	-0.000001928	-0.000001461	0.000003568	H	-0.000000458	-0.000006249	0.000001243
H	-0.000000476	-0.000004413	0.000007175	H	0.000003116	-0.000003892	0.000004957
H	-0.000001816	-0.000005318	0.000001728	H	-0.000002869	0.000001049	-0.000002612
H	-0.000001669	0.000002810	-0.000001104	H	-0.000002529	-0.000003698	-0.000003286
C	0.000041543	-0.000007852	0.000069608	C	0.000002945	0.000002102	-0.000001290
H	0.000008652	0.000005085	-0.000007841	H	0.000001062	0.000004991	0.000001971
H	0.000001189	0.000000410	-0.000009359	H	0.000000749	0.000004945	-0.000003326
S	-0.000044294	-0.000007344	-0.000008556	S	-0.000005239	0.000003041	0.000003024
H	-0.000007304	-0.000002417	0.000011098	H	0.000001173	0.000005680	-0.000000694
<b>2b</b>				<b>2b</b>			
C	-0.000006396	-0.000054276	-0.000008172	C	0.000007206	0.000020521	-0.000003255
C	-0.000033592	0.000022307	-0.000008913	C	0.000005253	-0.000021456	-0.000003885
C	0.000053993	0.000038625	0.000023838	C	-0.000001177	0.000001016	-0.000000132
C	-0.000000196	-0.000061642	-0.000001380	C	0.000004127	0.000003722	-0.000003292
C	-0.000038139	0.000019063	-0.000012212	C	0.000004919	0.000001203	0.000001179
C	0.000034483	0.000029946	0.000016547	C	-0.000016009	-0.000014445	-0.000001607
H	0.000001013	0.000004217	0.000000971	H	0.000000450	-0.000011539	-0.000005302
H	0.000002698	-0.000001086	-0.000001948	H	-0.000004590	-0.000000511	0.000002828
H	0.000000233	0.000000516	-0.000001738	H	-0.000003377	-0.000004571	-0.000001295
C	-0.000014556	0.000006994	0.000007293	C	-0.000005192	0.000002326	0.000011782
H	0.000003089	-0.000000582	-0.000000336	H	0.000001451	0.000003665	-0.000000532
H	0.000000678	0.000000652	-0.000005546	H	-0.000003086	0.000002667	0.000001087
S	0.000009493	0.000001736	-0.000005662	S	0.000000629	0.000008668	-0.000000826
H	-0.000001691	-0.000001615	0.000001105	H	0.000002189	0.000009493	0.000005173
H	-0.000011109	-0.000004856	-0.000003850	H	0.000007206	-0.000000759	-0.000001921
<b>2c</b>				<b>2c</b>			
C	-0.000024645	-0.000009053	0.000006404	C	0.000011178	-0.000007983	-0.000006690
C	0.000107145	0.000032045	0.000023447	C	-0.000018107	0.000001396	-0.000002026
C	-0.000050337	0.000006345	-0.000018948	C	0.000016189	0.000007977	-0.000008968
C	0.000037181	0.000019436	-0.000007771	C	-0.000012058	-0.000006061	0.000000904
C	-0.000037299	-0.000055832	-0.000010738	C	0.000005282	-0.000002703	-0.000001521
C	0.000052368	0.000014063	0.000003415	C	-0.000009804	0.000001225	-0.000002047
H	-0.000005150	0.000009355	0.000006429	H	-0.000001586	0.000000140	0.000004744
H	-0.000007032	0.000000555	0.000003645	H	-0.000001172	-0.000003486	-0.000002467
C	-0.000028187	0.000007192	-0.000024222	C	0.000010395	0.000001845	0.000016242
H	0.000004159	-0.000003515	0.000008575	H	0.000000906	0.000001612	-0.000000933
H	-0.000000909	0.000003331	0.000004524	H	0.000001017	0.000003037	0.000000998
S	-0.000005552	-0.000002999	0.000001632	S	-0.000002706	0.000001856	0.000003154
H	0.000002252	-0.000000819	0.000006884	H	-0.000001165	0.000002444	0.000006820
H	-0.000011199	0.000000105	0.000002513	H	-0.000000281	-0.000000225	-0.000000846
H	-0.000032792	-0.000020209	-0.000005790	H	0.000001912	-0.000001076	-0.000007365

<b>2d</b>				<b>2d</b>			
C	0.000002705	0.000016174	0.000003717	C	0.000013994	-0.000003638	0.000000000
C	0.000010173	-0.000013646	-0.000000409	C	-0.000013367	0.000012651	0.000000000
C	-0.000008518	0.000018387	0.000002232	C	0.000052774	0.000085853	0.000000000
C	-0.000025075	-0.000008446	-0.000001614	C	-0.000081029	-0.000059725	0.000000000
C	0.000016695	-0.000009962	-0.000003255	C	0.000065309	-0.000008186	0.000000000
C	-0.000016169	-0.000001595	-0.000004323	C	-0.000021130	-0.000010007	0.000000000
H	-0.000000607	-0.000001349	-0.000001421	H	0.000004372	-0.000008079	0.000000000
H	-0.000001595	0.000001742	-0.000000630	H	0.000015902	0.000001041	0.000000000
H	-0.000003329	0.000002153	0.000002050	H	-0.000024947	-0.000000454	0.000000000
H	0.000001106	0.000000559	0.000001727	H	0.000004902	-0.000008985	0.000000000
C	0.000033061	-0.000013835	0.000004944	C	0.000024828	0.000015581	0.000000000
H	-0.000005530	0.000004432	-0.000002422	H	-0.000072063	0.000021614	0.000000000
S	-0.000007176	0.000008728	0.000000248	S	0.000017204	-0.000049040	0.000000000
H	0.000000938	-0.000002608	-0.000001219	H	0.000011692	0.000018340	0.000000000
H	0.000003323	-0.000000735	0.000000374	H	0.000001557	-0.000006965	0.000000000
<b>2e</b>				<b>2e</b>			
C	-0.000025797	0.000010103	0.000000000	C	-0.000098642	-0.000154994	0.000000000
C	0.000026605	0.000002740	0.000000000	C	-0.000090008	-0.000114315	0.000000000
C	-0.000017498	-0.000015679	0.000000000	C	0.000254368	0.000102529	0.000000000
C	0.000007922	0.000002564	0.000000000	C	-0.000062596	-0.000198792	0.000000000
C	0.000016434	-0.000015981	0.000000000	C	-0.000164952	0.000186201	0.000000000
C	-0.000002099	-0.000010239	0.000000000	C	-0.000047942	0.000279383	0.000000000
H	0.000002054	0.000004125	0.000000000	H	-0.000023183	-0.000015639	0.000000000
H	0.000001856	0.000002322	0.000000000	H	0.000015889	-0.000035130	0.000000000
H	0.000001531	0.000005738	0.000000000	H	0.000023273	0.000025749	0.000000000
H	0.000001664	0.000002094	0.000000000	H	-0.000023676	-0.000001083	0.000000000
C	-0.000034283	0.0000123294	0.000000000	C	0.000599811	-0.000242192	0.000000000
H	-0.000005590	-0.000036848	0.000000303	H	-0.000142500	0.000107152	0.000024035
S	0.000032117	-0.000037870	0.000000000	S	-0.000141067	0.000012194	0.000000000
H	0.000000674	0.000000485	0.000000000	H	0.000043724	-0.000058216	0.000000000
H	-0.000005590	-0.000036848	-0.000000303	H	-0.000142500	0.000107152	-0.000024035
<b>TS<sub>1a-1b</sub></b>				<b>TS<sub>1a-1b</sub></b>			
C	-0.000000974	0.000000655	-0.000001068	C	0.000002540	-0.000000919	-0.000005195
C	-0.000000074	0.000002037	-0.000004386	C	0.000001701	-0.000003177	-0.000013418
C	0.000001888	-0.000001097	-0.000007478	C	-0.000001723	-0.000003116	-0.000014228
C	-0.000005495	0.000005659	-0.000003106	C	-0.000002782	-0.000004118	-0.000005560
C	0.000007350	0.000000466	-0.000000672	C	-0.000006560	-0.000001720	0.000001504
C	-0.000002063	-0.000001035	0.000000462	C	-0.000000786	0.000001223	0.000003625
H	-0.000001008	-0.000000047	0.000001042	H	0.000005242	0.000000023	-0.000005129
H	-0.000000508	0.000001658	-0.000005778	H	0.000004069	-0.000004062	-0.000019784
H	0.000000709	0.000002353	-0.000009647	H	-0.000001287	-0.000005576	-0.000020733
H	0.000001270	-0.000001536	-0.000001955	H	-0.000003942	0.000000495	0.000001540
C	-0.000000325	-0.000003128	0.000005823	C	0.000004133	0.000007085	0.000012140
H	0.000001100	-0.000002115	0.000006664	H	0.000008246	0.000005460	0.000012587
H	-0.000002034	-0.000001049	0.000006573	H	-0.000004042	0.000002143	0.000013939
O	0.000000345	-0.000001906	0.000008646	O	-0.000000135	0.000002583	0.000019967
H	-0.000000182	-0.000000914	0.000004880	H	-0.000004674	0.000003675	0.000018747
<b>TS<sub>1a-1e</sub></b>				<b>TS<sub>1a-1e</sub></b>			
C	-0.000000231	0.000001717	-0.000009881	C	0.000011854	0.000031335	0.000000000
C	0.000001012	0.000005497	0.000001654	C	0.000009583	0.000005882	0.000000000
C	0.000000535	0.000000458	-0.000001134	C	0.000046899	0.000000396	0.000000000
C	0.000006709	0.000000523	0.000002670	C	-0.000008715	0.000033119	0.000000000
C	-0.000003524	0.000003819	-0.000000450	C	0.000227299	-0.000040498	0.000000000
C	-0.000020354	-0.000000565	0.000015708	C	-0.000044650	-0.000050744	0.000000000

H	-0.000004945	0.000000964	-0.000000910	H	-0.000017888	0.000003692	0.000000000
H	-0.000001925	0.000005063	-0.000000711	H	-0.000009700	0.000023448	0.000000000
H	0.000003021	0.000005570	-0.000000509	H	0.000011243	0.000027422	0.000000000
H	0.000005406	0.000001836	0.000001941	H	0.000012493	0.000005477	0.000000000
C	-0.000009749	-0.000003838	-0.000014655	C	-0.000060531	0.000099469	0.000000000
H	-0.000009087	-0.000008277	0.000001479	H	-0.000003499	-0.000012254	0.000009847
H	0.000002666	-0.000001685	0.000005702	H	-0.000003499	-0.000012254	-0.000009847
O	0.000013056	0.000031299	0.000005381	O	-0.000205613	0.000034751	0.000000000
H	0.000017410	-0.000042382	-0.000006283	H	0.000034723	-0.000149241	0.000000000
<b>TS1b-1c</b>				<b>TS1b-1c</b>			
C	-0.000020805	-0.000001260	-0.000000143	C	0.000002913	-0.000002742	-0.000004914
C	0.000017322	-0.000008846	-0.000005346	C	0.000001144	-0.000005240	-0.000013067
C	0.000006098	0.000036766	0.000005078	C	-0.000001295	-0.000004352	-0.000013264
C	-0.000002722	-0.000034445	-0.000014659	C	0.000003125	-0.000007971	-0.000005071
C	-0.000023485	-0.000026967	-0.000005052	C	-0.000012813	0.000001682	0.000002606
C	0.000015505	0.000037039	0.000009769	C	0.000000372	0.000002688	0.000002824
H	0.000000043	-0.000000342	0.000001094	H	0.000005611	-0.000000727	-0.000004885
H	-0.000000408	0.000003196	-0.000006038	H	0.000004865	-0.000006715	-0.000019315
H	0.000001305	0.000003653	-0.000009730	H	-0.000000497	-0.000008330	-0.000019887
C	0.000000487	-0.000015162	-0.000006920	C	0.000000479	0.000004410	0.000012338
H	-0.000002705	-0.000011694	0.000005545	H	0.000007534	0.000006592	0.000012609
H	0.000004035	0.000006129	0.000004663	H	-0.000004157	0.000004542	0.000013260
O	-0.000005091	0.000004308	0.000026414	O	0.000001466	0.000009129	0.000017731
H	0.000005556	-0.000001451	0.000000322	H	-0.000005413	0.000006395	0.000018230
H	0.000004866	0.000009076	-0.000004997	H	-0.000003334	0.000000638	0.000000803
<b>TS2a-2b</b>							
C	0.000002147	-0.000016647	-0.000002956				
C	-0.000001041	0.000012651	0.000015655				
C	-0.000017589	-0.000013472	0.000000163				
C	0.000017278	0.000012255	0.000007973				
C	-0.000004906	0.000002584	-0.000007515				
C	0.000005719	0.000000180	-0.000003333				
H	-0.000000152	-0.000003637	0.000002025				
H	0.000002132	-0.000004399	0.000011543				
H	-0.000000507	0.000000369	-0.000010496				
H	-0.000000500	-0.000002622	-0.000008913				
C	-0.000001745	0.000002676	-0.000004015				
H	0.000000289	0.000007516	0.000005673				
H	0.000000327	0.000007033	-0.000005073				
S	-0.000001027	-0.000003592	0.000000226				
H	-0.000000425	-0.000000896	-0.000000957				
<b>TS2a-2d</b>							
C	0.000024212	-0.000101601	0.000008216				
C	-0.000077758	0.000058814	-0.000004030				
C	0.000146814	0.000253350	0.000012515				
C	-0.000244385	-0.000229038	0.000012061				
C	-0.000130578	0.000015211	-0.000076477				
C	0.000129146	0.000038383	0.000020962				
H	0.000001723	-0.000012421	0.000000957				
H	0.000001108	-0.000006406	0.000000902				
H	-0.000008263	0.000002118	0.000000097				
H	-0.000003438	-0.000005924	-0.000004446				
C	0.000125106	-0.000025543	-0.000018459				
H	0.000012576	-0.000017058	0.000047232				
H	-0.000003157	0.000003002	0.000000900				

S	0.000029129	0.000021292	0.000004172	
H	-0.000002236	0.000005820	-0.000004601	
<b>TS<sub>2a-2e</sub></b>				
C	0.000008013	-0.000015502	-0.000003979	
C	-0.000020837	0.000008665	0.000017531	
C	-0.000003886	-0.000018560	0.000009402	
C	0.000023790	0.000042689	0.000015751	
C	0.000004627	0.000014321	-0.000006058	
C	0.000003605	0.000012191	0.000006601	
H	-0.000001453	0.000001962	0.000006789	
H	0.000000979	-0.000001674	-0.000014406	
H	0.000002228	-0.000004553	0.000026533	
H	0.000002621	-0.000002294	0.000003615	
C	0.000004095	-0.000025573	0.000002550	
H	-0.000016567	-0.000000610	0.000004600	
H	0.000022136	0.000009421	-0.000002169	
S	-0.000014998	-0.000018751	-0.000016485	
H	-0.000014353	-0.000001732	0.000004325	
<b>TS<sub>2b-2c</sub></b>				
C	-0.000005540	0.000004982	-0.000001628	
C	-0.000008410	-0.000000153	-0.000007294	
C	0.000014886	0.000000412	0.000002387	
C	-0.000001315	0.000000335	0.000002998	
C	0.000000614	-0.000001991	0.000002919	
C	0.000004992	0.000002520	-0.000002799	
H	-0.000004512	-0.000007013	0.000002585	
H	0.000000169	-0.000000014	-0.000000738	
H	-0.000000047	-0.000000049	0.000000157	
C	-0.000001491	-0.000000504	0.000000963	
H	0.000000928	0.000000280	-0.000000422	
H	-0.000000247	0.000000794	-0.000000243	
S	0.000000305	0.000001525	-0.000001125	
H	0.000000375	-0.000001649	-0.000000032	
H	-0.000000706	0.000000526	0.000002273	